Toxicology Reports 14 (2025) 101882

Contents lists available at ScienceDirect

Toxicology Reports

journal homepage: www.elsevier.com/locate/toxrep

Podocyte-related biomarkers' role in evaluating renal toxic effects of silver nanoparticles with the possible ameliorative role of resveratrol in adult male albino rats

Eman El-Sayed Khayal [a], Mona G. Elhadidy [b,c,*], Sulaiman Mohammed Alnasser [d], Manal Mohammad Morsy [e], Azza I. Farag [e], Samah A. El-Nagdy [a]

[a] Department of Forensic Medicine and Clinical Toxicology, Faculty of Medicine, Zagazig University, Egypt
[b] Department of Medical Physiology, Faculty of Medicine, Mansoura University, Egypt
[c] Department of Medical Physiology, Faculty of Medicine, Al-Baha University, Saudi Arabia
[d] Department of Pharmacology and Toxicology,College of Pharmacy, Qassim University, Qassim 51452, Saudi Arabia
[e] Department of Human Anatomy and Embryology, Faculty of Medicine, Zagazig University, Egypt

ARTICLE INFO

Keywords:
Silver nanoparticles
Resveratrol
Podocin
Nephrin
Monocyte chemoattractant protein-1
TGF-β1and Claudin-1

ABSTRACT

Extensive uses of silver nanoparticles (Ag NPs) in different industries result in exposure to these nanoparticle imperatives in our daily lives. Resveratrol is found in many plants as a natural compound. The present study aimed to estimate the renal toxic effects of Ag NPs in adult male albino rats and the underlying relevant mechanisms while studying the possible role of resveratrol in ameliorating these effects. Thirty adult albino rats were split into 5 groups; control, vehicle, resveratrol (30 mg/kg), Ag NPs (300 mg/kg), and resveratrol + Ag NPs groups. The treatments were given orally for 4 weeks. Ag NPs group displayed a reduction in kidney weight (absolute and relative), excess in urinary levels of kidney injury molecule, neutrophil gelatinase-associated lipocalin, cystatin, and blood kidney biomarkers (creatinine, urea, and potassium), increases in oxidative stress markers with the reduction in antioxidant markers, and decreases in serum sirtuin 1(SIRT1) level. Upregulation of interleukin 1 beta, tumor necrosis factor-alpha, and monocyte chemoattractant protein-1 gene expressions with downregulation of nephrin and podocin gene expressions in renal tissues were also observed. These changes were associated with histological alterations of the glomeruli and tubules, and increased area percentage of collagen fiber. A significant increase in the optical density of *transforming growth factor-beta* 1 and claudin-1 immunostaining was detected in the Ag NPs group when compared to other groups. All these changes were alleviated by the usage of resveratrol through its anti-oxidant, anti-inflammatory, and activation of SIRT1 recommending its use as a renoprotective agent.

1. Introduction

There is a noticeable increase in the use of nanoparticles worldwide in different fields as industrial, and biomedical fields causing environmental contamination. As a result, several scientific researches are done progressively to ensure the safety and harmful effects of these nanoparticles. Among these widely used nanoparticles are silver nanoparticles (Ag NPs) [81,97].

Silver nanoparticles are characterized by unparalleled physicochemical characteristics as their nanoscale range (1–100 nm), high surface area, strong chemical reactivity and conductivity [15,61], making them to be used in various fields such as electronics, agrifoods, water purifications, cosmetics, and biomedical fields [46,71]. Exposure to Ag NPs can be through ingestion, inhalation, or skin contact [73]. After absorption, Ag NPs are distributed to different organs causing pathological changes [67,102]

Despite the several benefits of Ag NPs in the community, many environmental hazards escalate during their production, processing, utilization, and waste disposal [69,71].

The kidney is considered the primary organ of excretion. Moreover, it importantly regulates different hormones synthesis and release. It is seen to be an important target organ liable to adverse effects induced by

* Corresponding author at: Department of Medical Physiology, Faculty of Medicine, Mansoura University, Egypt
E-mail addresses: EAKhayal@medicine.zu.edu.eg (E.E.-S. Khayal), dr_monagaber@mans.edu.eg (M.G. Elhadidy), sm.alnasser@qu.edu.sa (S.M. Alnasser), MMOmmar@medicine.zu.edu.eg (M.M. Morsy), SAElnagdy@medicine.zu.edu.eg (S.A. El-Nagdy).

https://doi.org/10.1016/j.toxrep.2024.101882
Received 6 October 2024; Received in revised form 18 December 2024; Accepted 20 December 2024
Available online 27 December 2024

nanoparticles [72]. It is one of the organs that can be affected by the toxic effects of Ag NPs. Glomerular injury is critically regulated by podocytes which when injured can not be replaced or regenerated as they are terminally differentiated cells [54]. This injury can be monitored by assessment of nephrin and podocin which are podocyte proteins involved mainly in the maintenance of slit diaphragm structure [64].

Podocytes are terminally differentiated cells. Their loss can't be replaced or regenerated, which eventually induces glomerulosclerosis. So, glomerular injury is critically regulated by podocytes [54]. Nephrin and podocin are podocyte proteins that participate essentially in the maintenance of the structural safety of the slit diaphragm [64].

Other biomarkers that are involved in renal injury include MCP-1 and SIRT 1. MCP-1 is an important chemokine produced by glomerular mesangial cells and podocytes upon stimulation by various stimuli including inflammation [86]. Normally SIRT1 is present in the kidneys. Through many different physiological mechanisms, SIRT1 plays an effective role in maintaining the function of kidney cells [20]. SIRT1 is believed to protect against podocytopathy by regulating mitochondrial functions, nucleosome histone acetylation, and diverse transcriptional factor activities [38].

Resveratrol is a natural compound present in many plants like grapes, berries, peanuts, pine, and legumes. Recently, resveratrol has been recommended as a dietary supplement because of its beneficial effects on health [16]. These effects are related to its ability to protect against inflammation, aging, cancer, and free radicals causing oxidative stress, in addition to antiviral, antiplatelet, anti-mutagenic, cardioprotective, and hepatoprotective effects [77,100]. Many studies have demonstrated the protective effects of resveratrol in nephrotoxicity models induced by different chemicals such as cisplatin, carbon tetrachloride, and thioacetamide [24,28,100].

In light of this information, this scientific research aimed to evaluate renal toxic effects after oral administration of Ag NPs to adult male albino rats and the underlying relevant mechanisms while studying the possible role of resveratrol in ameliorating these effects.

2. Material and methods

2.1. Experimental animals

30 adult male Wistar albino rats with an average weight of 200–220 g (g) were collected from the animal breeding house of the Faculty of Medicine, Zagazig University. They were kept in 6 rats per cage supplied with commercial laboratory animal needs from food and water. The temperature was kept constant and suitable for rats. Under the number ZU-IACUC/3/F/157/2022, the Institutional Animal Care and Use of Zagazig University, Egypt approved this experimental protocol in accordance with applicable international laws and regulations encouraging the researchers to achieve their duties to perform animal experiments with the highest level of scientific, humane, and ethical rules [12].

2.2. Experimental design

The rats were left for seven days to adapt, and then sectioned into the following five equal groups; group I (control); nothing was added, except laboratory food and water, group II (vehicle); orally gavaged with 0.5 mL of distilled water once daily, 6 days /week for 4 weeks, group III [Resveratrol(Sigma-Aldrich, CAS No: 1185247–70–4)]; orally gavaged at a dose of 30 mg/kg once daily, 6 days /week for 4 weeks (Gelen and Şengül, 2021), group IV [Silver nanoparticles (Sigma-Aldrich, CAS No: 7440–22–4): brown odorless fine nano-powder with particle size < 100 nm and purity ≥ 99.5)]; orally gavaged with 300 mg/kg of Ag NPs [62] after being dissolved in 0.5 mL of distilled water once daily, 6 days/week for 4 weeks, group V (Resveratrol + Silver nanoparticles); each rat was gavaged orally with resveratrol and Ag NPs as same previous doses separated by one hour for 4 weeks.

The body weight of rats was measured at the start and the end of the study. One day before the necropsy, the rats were separated individually for 24 hours (one rat in each cage). Urine samples were gathered in clean containers and saved at the temperature of −20°C till urinary biomarkers analysis was done. On the day of the necropsy, blood samples were drawn from the retroorbital plexus of all rats anesthetized by using pentobarbitone sodium (50 mg/kg intraperitoneal single dose) according to method demonstrated by [63]. 7 mL of the blood samples were left for spontaneous coagulation, then passed on a centrifuge device at 2000 rpm for 20 minutes. The sera were collected and saved at −20 °C for estimating creatinine, urea, potassium level, sodium level, and SIRT1 levels.

Later on, both kidneys from each rat were removed after euthanizing them. Firstly the kidneys' weights of all studied rats [The absolute and relative weight (organ-to-body weight ratio)] were scaled. After that, one kidney was homogenized by adding in ice-cold lysis buffer and then centrifuged at 8000 x g for 20 min at 5℃. The homogenates were collected and used for detecting oxidative stress, inflammatory markers, nephrin, podocin, and monocyte chemotactic protein-1 (MCP-1) expression. Histopathological and immunohistochemical examination of the other kidney was done. Fig. 1

2.3. Silver nanoparticles characterization

Silver nanoparticles were examined under transmission electron microscopy (TEM) at the Electron Microscope Unit, Faculty of Agriculture, Mansoura University, Egypt. An aqueous dispersion of the Ag NPs was dropped onto a carbon-coated copper grid and left to dry in the air (Fig. 2).

2.4. Blood and urine renal injury biomarkers assessment

The sera were utilized to assess the following:

- Serum creatinine by colorimetric method as described by [84].
- Serum urea by colorimetric method as described by [48].
- Serum potassium (K^+) and sodium (Na^+) levels were determined according to [21] consuming commercial tools (Sensacore electrolyte, Andhra Pradesh, India).

Stored urine samples were used to estimate *the following:*

- Urine KIM-1 was measured by ELISA using the commercially available kit (R&D Systems, Minneapolis, MN, USA) and following the manufacturer's instructions.
- Urine NGAL was measured using an ELISA kit (BioPorto, Denmark) by method following the manufacturer's instructions.
- Urine cystatin C was measured using an ELISA kit (R&D Systems, Minneapolis, MN, USA) by method following the manufacturer's instructions.
- The data of KIM-1, NGAL, and cystatin C were expressed by (ng/mL).

2.5. Serum SIRT1 level

The serum level of SIRT1 was measured by (ELISA) using the commercially available kit (Catalog #MBS2600246, MyBioSource).

2.6. Biochemical analyses of renal tissue homogenates

2.6.1. Oxidative stress markers evaluation

- Protein carbonyl assay was determined by spectrophotometry as demonstrated by [49]. The expression unit was nmol/mg protein.
- Renal xanthine oxidase activity was determined by spectrophotometry as demonstrated by [66] and expressed as mU/min/g of tissue.

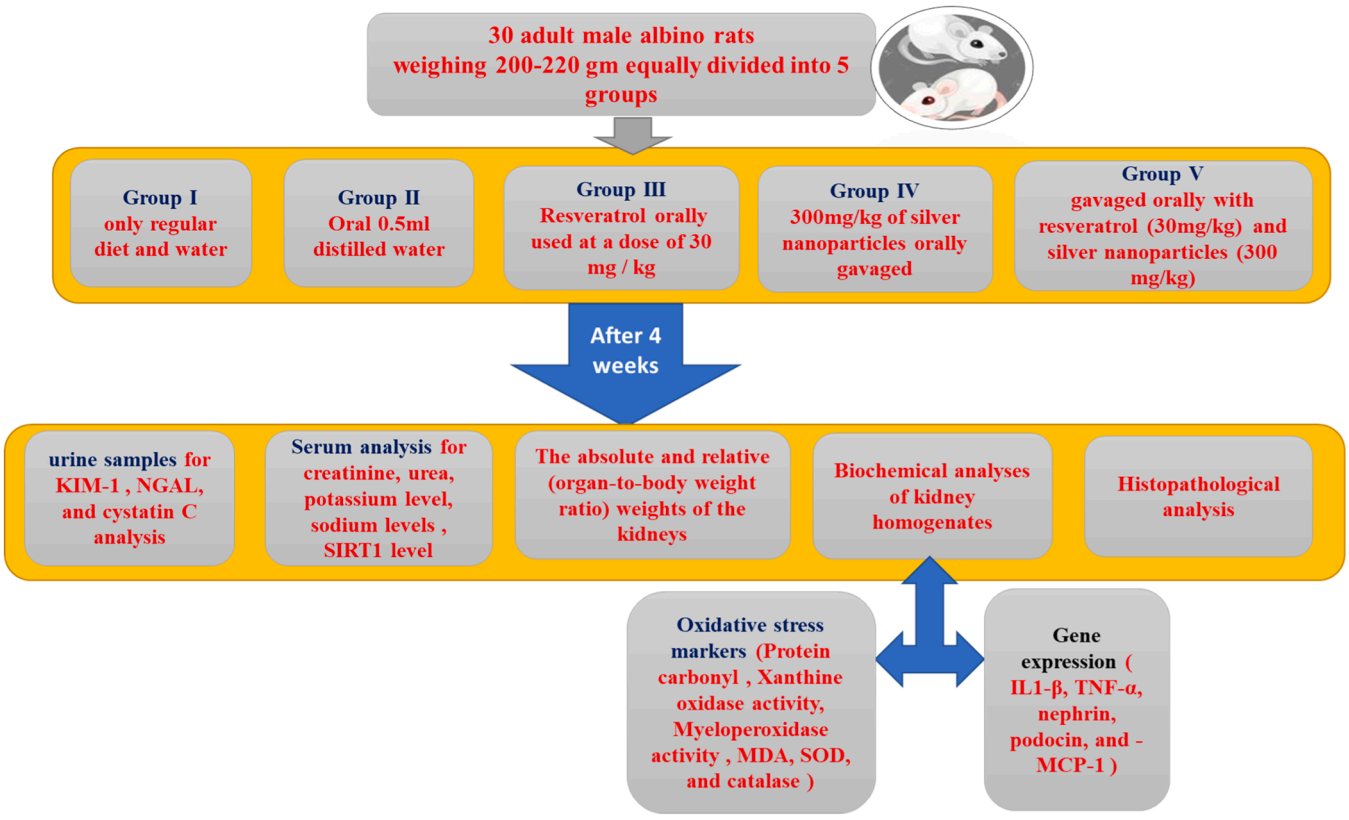

Fig. 1. Experimental design.

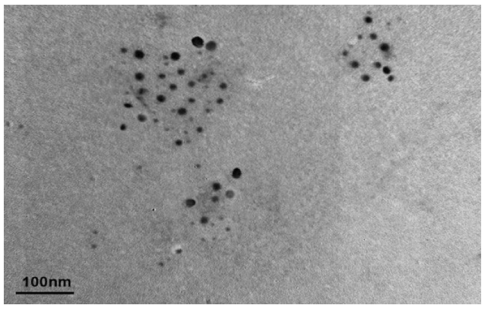

Fig. 2. Silver nanoparticles characterization by transmission electron microscope.

- Myeloperoxidase activity in the kidney was assessed by spectrophotometry as determined by [91], and expressed as U/min/mg protein.
- Renal MDA assay was measured following the method of [75]. The expression unit was nmol/mg protein.
- Superoxide dismutase (SOD) activity was assessed by the method of [55]. The expression unit was U/g protein.

- Catalase activity was measured by spectrophotometer at 240 nm according to [2]. The expression unit was U/g tissue.

2.6.2. Gene expression in kidney homogenates

IL1-β, TNF-α, nephrin, podocin, and MCP-1 gene expression analysis by real-time polymerase chain reaction (RT PCR) were done as follows: RNA was extracted from kidney homogenate by using Qiagen RNA isolation kit (RNeasy; Qiagen Ltd, Crawley, West Sussex, UK) following the manufacturer's instruction. The total RNA amount was recognized by a spectrophotometer by scaling the absorbance at 260 nm. After that, RNA reverse transcription was done using the available kit (Quantitect Reverse Transcription Kit, Qiagen, Cat. No. / ID: 205311). Later on, reverse transcription PCR was performed using QuantiFast SYBR Green RT-PCR Kit, Qiagen, Cat. No. / ID: 204156 following the manufacturer's protocol. The primer sequences for IL1-β, TNF-α, nephrin, podocin, and MCP-1 markers were tabulated in Table 1.

2.7. Histopathological analysis

2.7.1. Hematoxylin and eosin staining

The kidney tissues fixed in formalin solution were embedded in paraffin blocks and used to prepare 5 μm thickness sections. These sections were stained by H & E stains according to the method designated by [6] and later examined by light microscopy. The kidney histopathological scoring was applied by histopathological evaluation of the kidney cortex in hematoxylin and eosin stained section. The score

Table 1
Primer sequences for IL1-β, TNF-α, nephrin, podocin, and MCP-1 markers by the RT-PCR analyses.

Gene	Accession number	Primer sequence
IL-1β	NM_031512.2	**Forward:** 5′GGCTTCCTTGTGCAAGTGTC3′ **Reverse:** 5′CACACACTAGCAGGTCGTCA3′
TNF-α	NM_012675.3	**Forward:** 5′GGCTTTCGGAACTCACTGGA3′ **Reverse:**5′CCCGTAGGGCGATTACAGTC3′
Podocin	NM_130828.3	**Forward:**5′GCTGTCTGCTACTACCGCAT3′ **Reverse:**5′TCACTGAGTCCAAGGCAACC3′
Nephrin	NM_022628.1	**Forward:**5′AACCGAGCCAAGTTCTCCTG 3′ **Reverse:**5′ GGACGACAAGACGAACCAGT 3′
MCP−1	NM_019190.1	**Forward:**5′ACAGGACCCTTCGTTTGGC3′ **Reverse:**5′CATCTTGCTGCAGATACATTTCAT3′
GAPDH	NM_001037190	**Forward:** 5′AGC CAG CTG TTG ACT TTG ATCG3′**Reverse:** 5′ACA TAC TCA GCA CCA GCG TC 3′

consisted of 4 separate components: *Glomerular, Tubular*, *Blood vessels* and *Interstitial*. The glomerular score was designed according to the degree of glomerular shrinkage and widening of Bowman's space: grade 0 (none), grade 1 (mild), grade 2 (moderate) or grade 3 (sever). *Tubular* score was applied as: grade 0 (no tubular dilatation), grade 1 (dilatation of 25 % of tubules), grade 2 (dilatation of 50 % of tubules) or grade 3 (dilatation of 75 % of tubules). Blood vessels score was done according to congestion and dilatation of blood vessels: grade 0 (no), grade 1 (slightly congested and dilated), grade 2 (moderately congested and dilated), grade 3 (marked congested and dilated). Regarding Interstitial mononuclear infiltrations, it was applied as: grade 0 (no infiltration), grade 1 (infiltration).

A total histopathological score (maximum 10) was obtained from the sum of the mean scores of the all variables. For achieving correct score, the same investigator examined all the samples. The mean value of each group was used for statistical analysis Table 2.

2.7.2. Masson's trichrome staining

5 μm-thick paraffin sections were cut from these paraffin-embedded tissue blocks, deparaffinized by immersing in xylene, rehydrated, and stained with Masson's trichrome staining for detection of fibrosis and collagen deposition [27,6].

2.8. Immunohistochemical study for claudin 1

Kidney tissue sections fixed in paraffin were deparaffinized and rehydrated using a series of graduated ethanol concentrations. After that, an autoclave for 10 minutes to extract the antigen was done. In order to prevent nonspecific protein binding, endogenous peroxidase activity was blocked using Protein Block Serum-Free (Dako, Japan) and T3 % hydrogen peroxidase. Rabbit polyclonal anti-claudin-1 (ab15098, Abcam, Cambridge, UK) was the primary antibody used, and it was diluted at a dilution of 1: 200 in Dako REAL Antibody Diluent. Subsequently, the sections were incubated at room temperature for one hour with the primary antibody. After that, the slides were cleaned three times using phosphate-buffered saline (PBS) and then for thirty minutes using an anti-rabbit antibody. Subsequently, 3,3′-diaminobenzidine (Dako kit, Agilent Technologies Inc., Santa Clara, CA) was applied to the sections, and Mayer hematoxylin was used as a counterstain [35,44].

2.9. Immunohistochemical study for TGF-β1

Rat renal cortex TGF-β1 immunolocalization was performed using the streptavidin-biotin complex method. Rat kidneys immersed in paraffin and fixed with formalin were sectioned at a 5 mm thickness on slides coated with poly-L-lysine. In 3 % H2O2 in methanol, the slices were rehydrated and then blocked against endogenous peroxidase activity. The sections were blocked with 5 % normal goat serum following the recovery of the antigen using a microwave and citrate buffer. Furthermore, to eliminate more endogenous biotin, the avidin/biotin blocking procedure was applied. After being diluted 1 in 2000 in phosphate-buffered saline, the TGF-β1 primary antibody (Boster, China) was incubated for 4 hours at room temperature. Horseradish peroxidase streptavidin was added after goat anti-rabbit biotinylated secondary antibody. The DAB-substrate chromogen method was utilized for visualization. PBS or IgG fractions from rabbit serum were used as negative controls in place of the main antibody. A cytoplasmic brown hue was the positive response to TGF-β1 protein production [35].

Table 2
kidney cortex scoring.

Pathological Lesion	Degree	Score
Glomerular shrinkage and widening of Bowman's space	none	0
	Mild	1
	Moderate	2
	Sever	3
Tubular dilatation	No	0
	Dilatation of 25 % of tubules	1
	Dilatation of 50 % of tubules	2
	Dilatation of 75 % of tubules	3
Blood vessels dilatation and congestion	No	0
	Slightly congested and dilated	1
	Moderately congested and dilated	2
	Marked congested and dilated	3
Interstitial mononuclear infiltrations	No	0
	Present	1

2.10. Morphometrical study

The area percentage % of collagen fiber was measured in Massion's Trichrome. The optical density (OD) of TGF-β1 & Claudin-1 protein expression was measured in TGF-β1 & Claudin-1 immune-histochemical stained sections respectively, using the objective lens of magnification X40. From each animal 6 randomly chosen, non-overlapping microscopic fields were examined. Image J Software was used for quantitative analysis in the anatomy department, faculty of medicine, Zagazig University [57].

3. Statistical analysis

It was done using SPSS software version 26 and GraphPad Prism version 9. Data expression was done with mean values ± standard deviations (SD). A post hoc least significant difference test (LSD test) was conducted after a one-way ANOVA (F) test. The total histopathological scoring was analysed by using The Kruskal-Wallis nonparametric one-way ANOVA. Dunn's multiple comparisons were then performed. Measurement of the direction and intensity of the association between two distinct variables was done using the Pearson Correlation coefficient. For all tests, if a p-value was less than 0.05, the difference was considered significant.

4. Results

No observed changes were detected between the control, vehicle, and resveratrol groups ($p > 0.05$) regarding all biochemical parameters measured in this experimental study, so, the control group (I) was compared with other examined groups.

4.1. Body weight

At the end of the study, significant reductions in body weight were observed in group (IV) taken Ag NPs, and group (V) taken combined resveratrol and Ag NPs compared to the control group ($p < 0.001$). Comparing the Ag NPs group with the resveratrol+Ag NPs group showed a significant increase in final body weight in group V ($p < 0.05$), Table 3.

4.2. Absolute and relative kidney weight

Significant reductions in absolute and relative kidney weight in group (IV) orally gavaged with Ag NPs and group (V) gavaged with combined resveratrol and Ag NPs for 4 weeks were noticed when compared with the control group (I) ($p < 0.001$). Comparing the Ag NPs group with the resveratrol+Ag NPs group showed significant increases in absolute and relative kidney weight in group V ($p < 0.001$, $p < 0.05$ respectively), Table 3.

Table 3
Comparison of mean values of initial and final body weight, absolute and relative kidney weight among studied groups by analysis of variance and least significant difference test.

Index	Control mean ± SD	Vehicle mean ± SD	Resveratrol mean ± SD	Silver nanoparticles mean ± SD	Resveratrol + Silver nanoparticles mean ± SD	F test	P values
Initial Body weight (8)	212.85 ± 6.25	211.93 ± 3.95	211.43 ± 6.31	213.09 ± 5.14	214.23 ± 2.91	0.27	0.89
Final Body weight (g)	229.013 ± 4.83	233.27 ± 5.01	231.6 ± 1.58	208.25 ± 2.15[a]	215.19 ± 3.12[a,c]	57	< 0.0001
Absolute kidney weight (g)	1.66 ± 0.038	1.67 ± 0.041	1.68 ± 0.019	1.22 ± 0.017[a]	1.42 ± 0.02[a,b]	296.5	< 0.0001
Relative weight of the kidney	0.725 ± 0.02	0.715 ± 0.01	0.725 ± 0.01	0.585 ± 0.048[a]	0.66 ± 0.015[a,c]	34.92	< 0.0001

Values are expressed as means ± standard deviation (n = 6)
[a] : highly significant difference as compared to the control group ($p < 0.001$),
[b] **:** highly significant difference as compared to the Ag NPs group ($p < 0.001$)
[c] : significant difference as compared to the Ag NPs group ($p < 0.05$)

4.3. Blood and urine renal injury biomarkers

Regarding *blood renal injury* biomarkers, Table 4 exhibited obvious increases in serum levels of creatinine, urea, and potassium with a decrease in serum level of sodium in the Ag NPs group and resveratrol + Ag NPs compared to those of the control group ($p < 0.001$). Comparing the resveratrol + Ag NPs group (V) with the control group showed rises in serum levels of creatinine, urea, and potassium ($p < 0.001$) and a lowering in serum levels of sodium ($p < 0.05$)**.**

Urine renal injury biomarkers (KIM-1, NGAL, and cystatin C) levels in group (IV) showed significant raises when these results were statistically compared to those of the control group (I) ($p < 0.001$). Usage of resveratrol with Ag NPs offered protection against these increases observed in group (IV) ($p < 0.001$), but this protection was partial as these changes were still significantly high compared with the results of control group (I) ($p < 0.001$), Table 4.

4.4. Serum SIRT1 level

Group (IV) taking Ag NPs for 4 weeks displayed a decrease in the mean values of serum SIRT1 level compared to the control group ($p < 0.001$). Furthermore, a reduction in serum SIRT1 level was detected significantly in the resveratrol + Ag NPs group compared to the control group ($p < 0.001$). Comparing the Ag NPs group with resveratrol + Ag NPs group showed significant protection of resveratrol against the reduction in mean values of serum SIRT1 level ($p < 0.001$), Fig. 3.

4.5. Biochemical analyses of kidney homogenates

Fig. 4 revealed obvious increases in levels of protein carbonyl, myeloperoxidase activity, and MDA in kidney homogenates in group (IV) concerning the control group (I) ($p < 0.001$). Comparing group (V) with group (I), statistically significant increases in levels of protein carbonyl, myeloperoxidase activity, and MDA were detected in group (V) ($p < 0.001$), however, comparison between group (IV) and group (V) showed a statistically significant reduction in these levels in group (V) ($p < 0.001$).

Fig. 5 showed an obvious increase in the mean values of xanthine oxidase activity and an obvious decrease in levels of superoxide dismutase and catalase activity in group (IV) and group (V) concerning the control group (I) ($p < 0.001$). On the other hand, a comparison between group (IV) and group (V) showed a significant reduction in xanthine oxidase activity and a significant increase in levels of superoxide dismutase and catalase activity in group (V) ($p < 0.001$).

4.6. Gene expression in kidney homogenates

Significant upregulation of IL1-β and TNF-α gene expressions was detected in the Ag NPs group (IV) and resveratrol + Ag NPs group (V) compared to the control group (I) ($p < 0.001$). In comparing group (IV) with group (V), the administration of resveratrol with Ag NPs in group (V) protected against these upregulations ($p < 0.001$), Fig. 6**.**

Regarding nephrin, podocin, and MCP-1, there was significant downregulation of nephrin and podocin gene expressions with

Table 4
Comparison of mean values of serum levels of creatinine, urea, potassium, sodium, and urine levels of KIM-1, NGAL, and cystatin C among studied groups by analysis of variance and least significant difference test.

Index	control mean ± SD	Vehicle mean ± SD	Resveratrol mean ± SD	Silver nanoparticles mean ± SD	Resveratrol + Silver nanoparticles mean ± SD	F test	P values
Serum creatinine (mg/dL)	0.74 ± 0.019	0.74 ± 0.012	0.75 ± 0.028	2.84 ± 0.17[a]	1.14 ± 0.07[a,b]	681.8	< 0.0001
Serum urea(mg/dL)	29.82 ± 0.94	30.09 ± 1.07	29.94 ± 0.85	67.34 ± 0.62[a]	44.99 ± 0.54[a,b]	2344	< 0.0001
Serum potassium level (mmol/L)	3.75 ± 0.14	3.84 ± 0.21	3.79 ± 0.17	5.53 ± 0.11[a]	4.52 ± 0.12[a,b]	144.8	< 0.0001
Serum sodium level (mmol/L)	136.79 ± 1.32	137.05 ± 0.08	136.92 ± 0.93	126.18 ± 2.79[a]	134.91 ± 0.26[c,b]	59.35	< 0.0001
Urine KIM−1 (ng/mL)	0.67 ± 0.06	0.67 ± 0.04	0.65 ± 0.05	4.82 ± 0.24[a]	2.61 ± 0.33[a,b]	594.9	< 0.0001
Urine NGAL (ng/mL)	0.91 ± 0.08	0.89 ± 0.04	0.91 ± 0.05	3.07 ± 0.17[a]	1.50 ± 0.02[a,b]	643.0	< 0.0001
Urine cystatin C (ng/mL)	0.62 ± 0.04	0.62 ± 0.03	0.62 ± 0.03	15.13 ± 0.48[a]	4.66 ± 0.12[a,b]	4710	< 0.0001

Values are expressed as means ± standard deviation (n = 6)
KIM-1: kidney injury molecule-1
NGAL: neutrophil gelatinase-associated lipocalin
[a] : highly significant difference as compared to the control group ($p < 0.001$),
[b] **:** highly significant difference as compared to the Ag NPs group ($p < 0.001$)
[c] : significant difference as compared to the control group ($p < 0.05$)

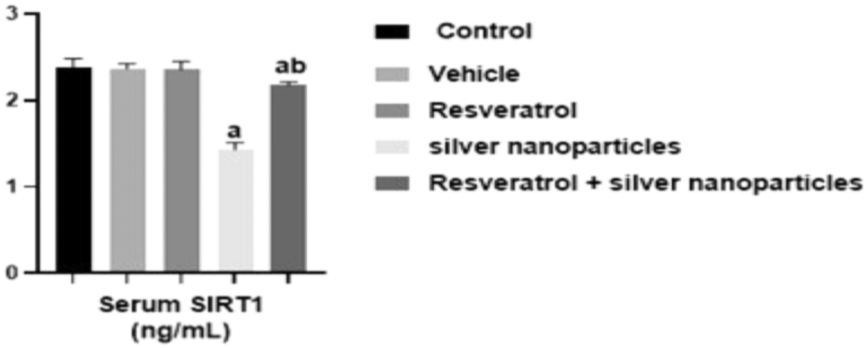

Fig. 3. Effect of silver nanoparticles on serum SIRT1 level among different studied groups, and role of resveratrol. Values are presented as the mean ± standard deviation (SD) in each treatment. **a**: $p < 0.001$ compared to the control group, **b**: $p < 0.001$ compared to the silver nanoparticles group.

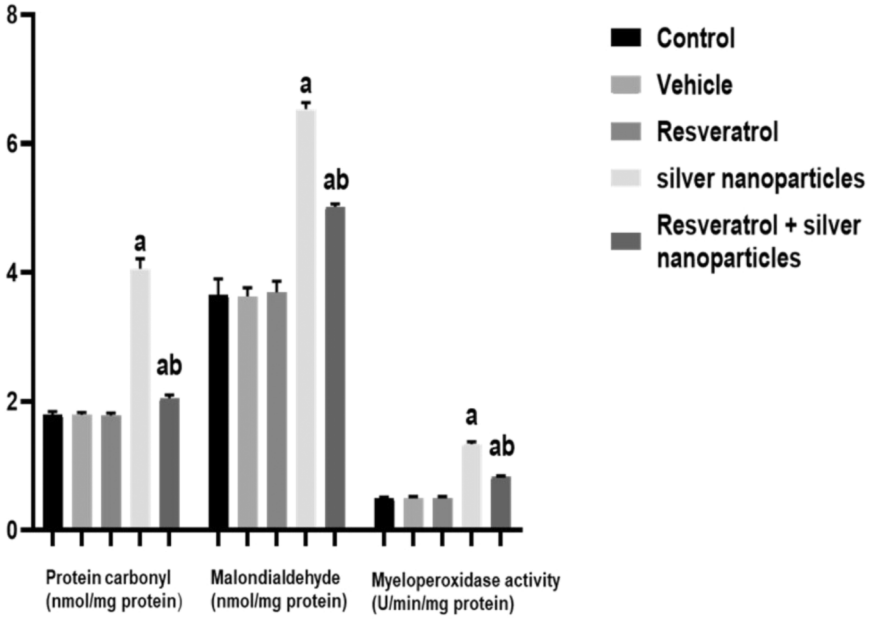

Fig. 4. Effect of silver nanoparticles on levels of protein carbonyl, malondialdehyde, and myeloperoxidase activity in kidney homogenates among different studied groups, and role of resveratrol. Values are presented as the mean ± standard deviation (SD) in each treatment. **a**: $p < 0.001$ compared to the control group, **b**: $p < 0.001$ compared to the silver nanoparticles group.

significant upregulation of MCP-1gene expression in Ag NPs group (IV) and resveratrol + Ag NPs group (V) compared to the control group (I) ($p < 0.001$). In comparing group (IV) with group (V), the administration of resveratrol with Ag NPs in group (V) protected against these changes ($p < 0.001$), Fig. 7.

A positive correlation was significantly found between serum SIRT1 level, podocin, and nephrin gene expression in kidney homogenates. In addition, a significant negative correlation was detected between serum SIRT1 level and MCP-1 ($p < 0.001$), Fig. 8.

According to Table 5, oxidative stress markers (MDA, protein carbonyl, xanthine oxidase activity, and myeloperoxidase activity) had significant negative correlations with podocin and nephrin and positive correlations with MCP-1($p < 0.001$). While superoxide dismutase and catalase showed positive correlations with podocin and nephrin and negative correlations with MCP-1($p < 0.001$).

Correlation studies between pro-inflammatory cytokines (IL1-β, TNF-α), podocin, nephrin, and MCP-1 revealed significant negative correlations between podocin and pro-inflammatory cytokines (IL1-β, TNF-α) in kidney homogenates. Similarly, significant negative correlations between nephrin and pro-inflammatory cytokines (IL1-β, TNF-α) were observed. In addition, there were significant positive correlations between MCP-1 and pro-inflammatory cytokines (IL1-β, TNF-α) ($p < 0.001$), Fig. 9.

4.7. Histological results

The control and vehicle control groups showed no obvious differences regarding all histological results. So, for comparison with other groups, the control group (I) was used.

Hematoxylin and Eosin (H&E) stained sections from control and resveratrol treated groups (groups I & III respectively) revealed the normal typical architecture of renal cortex that included renal corpuscles, proximal (PCT), distal convoluted tubules (DCT), and a little amount of the interstitial tissue. The renal corpuscles appeared composed of a glomerular tuft of capillaries surrounded by Bowman's capsule that formed of two layers; outer and inner separated by a clear Bowman's space. The outer parietal features flat epithelial cells while the inner visceral layer is made up of podocytes. The proximal convoluted tubules appeared with narrow lumen and lined with a single layer of high cuboidal epithelium that had deeply eosinophilic cytoplasm and rounded vesicular nuclei. Distal convoluted tubules exhibited broad lumen and were covered in low cuboidal epithelium that had rounded

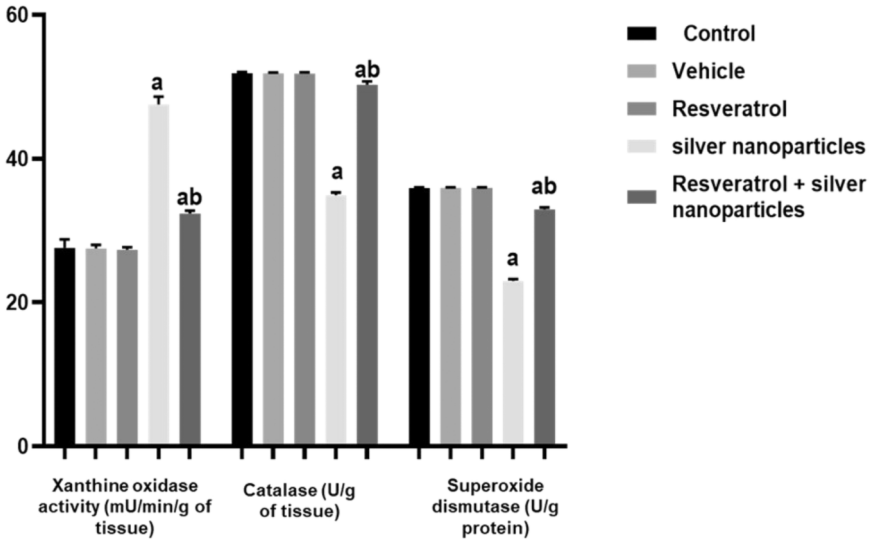

Fig. 5. Effect of silver nanoparticles on levels of xanthine oxidase, catalase, and superoxide dismutase in kidney homogenates among different studied groups, and role of resveratrol. Values are presented as the mean ± standard deviation (SD) in each treatment. a: $p < 0.001$ compared to the control group, b: $p < 0.001$ compared to the silver nanoparticles group.

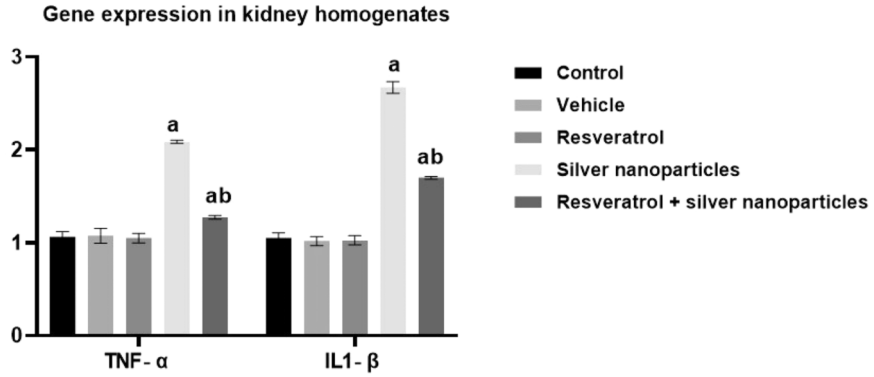

Fig. 6. Effect of silver nanoparticles on gene expression of IL1-β and TNF-α in kidney homogenates among different studied groups, and role of resveratrol. Values are presented as the mean ± standard deviation (SD) in each treatment. a: $p < 0.001$ compared to the control group, b: $p < 0.001$ compared to the silver nanoparticles group.

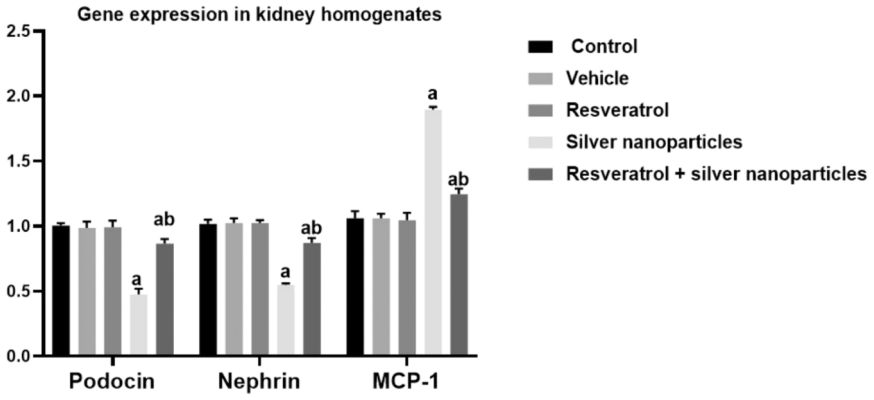

Fig. 7. Effect of silver nanoparticles on gene expression of podocin, nephrin, and MCP-1in kidney homogenates among different studied groups, and role of resveratrol. Values are presented as the mean ± standard deviation (SD) in each treatment. a: $p < 0.001$ compared to the control group, b: $p < 0.001$ compared to the silver nanoparticles group.

apical nuclei and pale eosinophilic cytoplasm, Fig. 10 A, B.

Sections of the renal cortex of the Ag NPs group (group IV) showed alterations in the glomeruli and tubules. Renal corpuscles demonstrated marked glomerular shrinkage, atrophy accompanied by loss of their vascular component and widening of the Bowman's space. The renal tubules revealed considerable dilatation with flatting of their epithelial

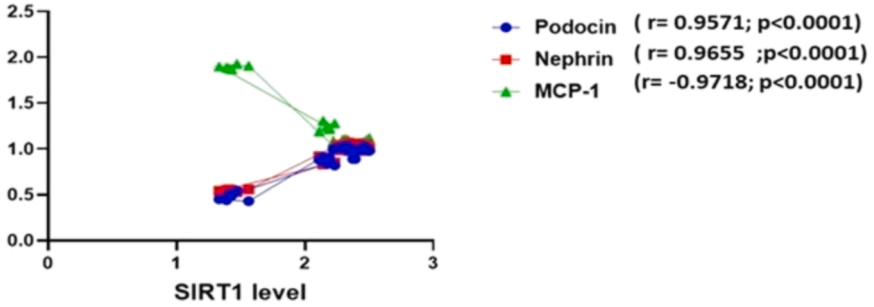

Fig. 8. Correlation Coefficient between serum SIRT1 level, podocin, nephrin, and MCP-1 gene expressions in kidney homogenates. Number of rats = 30.

Table 5
Correlation Coefficient between oxidative stress markers, podocin, nephrin, and MCP-1 gene expressions in kidney homogenates.

Variable	MDA (nmol/mg protein)		Protein carbonyl (nmol/mg protein)		Xanthine oxidase activity (mU/min/g of tissue)		Myeloperoxidase activity (U/min/mg protein)		Superoxide dismutase (U/g protein)		Catalase activity (U/g tissue)	
	R	P value	r	P value	r	P value	r	P value	r	P value	r	P value
Podocin	−0.956	< 0.0001	−0.969	< 0.0001	−0.976	< 0.0001	−0.963	< 0.0001	0.982	< 0.0001	0.969	< 0.0001
Nephrin	−0.966	< 0.0001	−0.965	< 0.0001	−.980	< 0.0001	−0.986	< 0.0001	0.986	< 0.0001	0.963	< 0.0001
MCP−1	0.948	< 0.0001	0.983	< 0.0001	0.983	< 0.0001	0.976	< 0.0001	- 0.99	< 0.0001	−0.983	< 0.0001

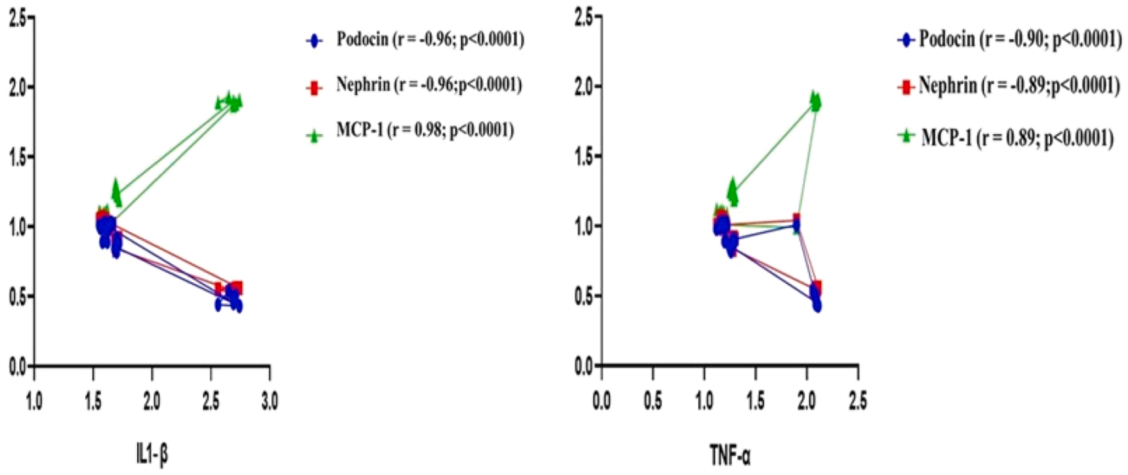

Fig. 9. Correlation Coefficient between IL1-β, TNF-α, podocin, nephrin, and MCP-1 gene expressions in kidney homogenates. Number of rats = 30.

lining that showed degeneration with pyknotic nuclei. Some tubules exhibited sloughing of either nuclei or epithelial cells from the basement membrane into their lumen. The interstitial blood vessels in between renal tubules were congested, and some showed marked dilatation with the detection of mononuclear infiltrations in the interstitial tissue, Fig. 10 C, D, and E.

On the other hand, group V (resveratrol + Ag NPs) showed noticeable improvement, displaying nearly normal renal corpuscles, PCT, and DCT. Similar to the control group, the renal glomerulus appeared formed of a glomerular tuft of blood capillaries with distinct regular Bowman's space. The lining epithelial cells of proximal tubules were high cuboidal demonstrating eosinophilic cytoplasm with vesicular basal nuclei. In addition, the lining epithelial cells of the distal tubule appeared low cuboidal cells demonstrating apical vesicular nuclei. However, it was found that a few tubules still had cystic dilatation, and a few epithelial cells with pyknotic nuclei were still seen in certain convoluted tubules, Fig. 10 F.

The control and resveratrol groups (groups I & III) demonstrated minimal amounts of collagen fibers around glomerular capillaries, Bowman's capsule, and renal tubules appearing as green-stained streaks, Fig. 11 A, B. However, rats treated with Ag NPs (group IV) exhibited high collagen fiber deposition, especially within the glomerulus, peritubular, and interstitial tissue around blood vessels when compared to the previous groups, Fig. 11 C, D. While the group V (resveratrol + Ag NPs) exhibited a nearly normal distribution of collagen fibers, Fig. 11 E.

The mean area % of collagen fiber in Massion's Trichrome stained sections from Ag NPs treated rats (group IV) revealed a significant ($p < 0.05$) increase in comparison with control, vehicle, and resveratrol groups. While the resveratrol + Ag NPs group showed a significant ($p < 0.05$) decrease in collagen deposition as compared with group IV, Fig. 11 F.

4.8. Histopathological scoring results

The kidney cortex sections of the silver nanoparticles treated group showed statistically significant increases in the degree of kidney affection in terms of *Glomerular* shrinkage and widening of Bowman's space, *Tubular dilatation*, *Blood vessels* dilatation and congestion and *Interstitial* mononuclear infiltrations. However the administration of resveratrol with Ag NPs in group (V) protected against these histopathological

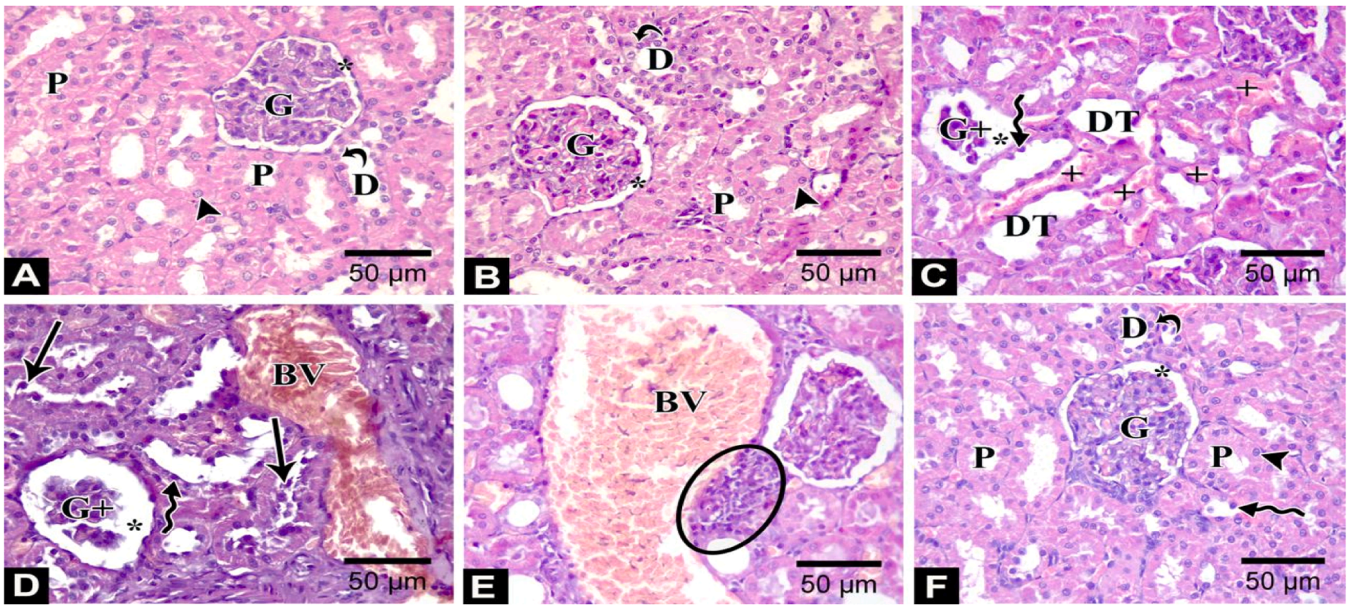

Fig. 10. Photomicrographs of sections of the renal cortex of the different studied groups; (A, B): The control and resveratrol groups respectively show renal corpuscles (G) with narrow Bowman's space (*), proximal convoluted tubules (P) lined by high cuboidal epithelium with rounded vesicular nuclei (arrowhead), distal convoluted tubules (D) lined low cuboidal epithelium that had rounded apical nuclei (curved arrow). (C-E): The Ag NPs group showed glomerular atrophy (G+) with widening of the Bowman's space (*), dilated renal tubules (DT) lined with flat epithelial cells (zigzag arrow), sloughed pyknotic nuclei or epithelial cells (arrow), congested peritubular blood vessels (+) and dilated congested interstitial blood vessels (BV) with mononuclear infiltrations in the interstitial tissue (lined oval area). (F) The resveratrol + Ag NPs group showed normal renal corpuscles (G) with narrow Bowman's space (*), proximal convoluted tubules (P) with an epithelial cell having vesicular nuclei (arrowhead), distal convoluted tubules (D) with apical nuclei (curved arrow) and some tubules still had pyknotic nuclei (zigzag arrow). (H & E, X 400; scale bar, 50 μm).

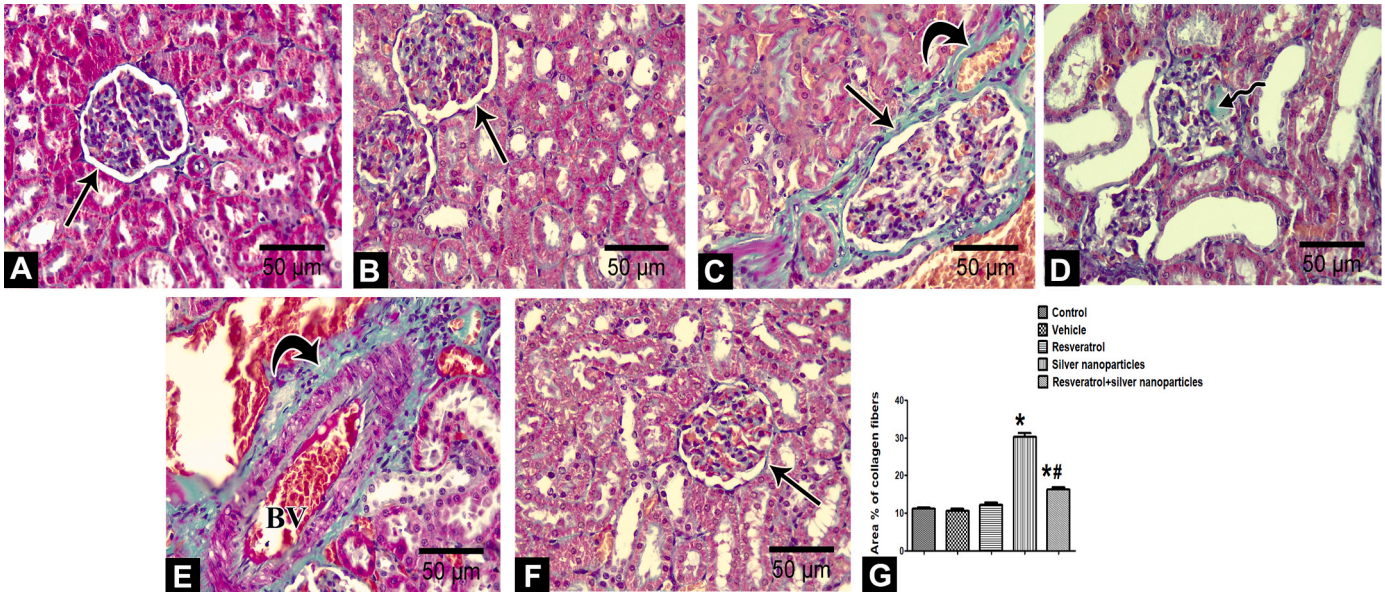

Fig. 11. Photomicrographs of renal cortex sections of different groups; (A, B): The control and resveratrol groups respectively showed minimal amounts of collagen fibers surrounding the glomeruli (arrow). (C-E): The Ag NPs group showed high collagen fiber deposition within the glomerulus (zigzag arrow), around glomeruli (arrow), and in the interstitial tissue around blood vessels (curved arrow). (F) The resveratrol + Ag NPs group showed a nearly normal distribution of collagen fibers around the glomerulus (arrow). (Masson trichome, x 400; scale bar 50 μm). (G) Effect of Ag NPs on collagen deposition in the renal cortex among different studied groups, and role of resveratrol. Values are presented as the mean ± standard deviation (SD) in each treatment. * : $p < 0.05$ compared to control, vehicle and resveratrol groups, #: $p < 0.05$ compared to silver nanoparticles group.

parameter ($p < 0.001$) Table 6.

4.9. Immunohistochemical results

Regarding TGF-β1 immune-marker expression, groups I and III (control & resveratrol groups) showed negative expression of TGF-β1 in the glomeruli and epithelial cells of the tubules, Fig. 12A, B. Group IV (Ag NPs) revealed strong positive cytoplasmic TGF-β1 immunostaining in the form of brown stains distributed in the cytoplasm of glomerular and epithelial cells of distal convoluted tubules. Also, a heavy brown

Table 6
Statistical evaluation of mean values of the kidney histopathological scoring in the studied groups.

Rat number	Control	Vehicle	Resveratrol	Silver nanoparticles	Resveratrol + Silver nanoparticles	Kruskal-Wallis test	P value
1	1	0	0	5	1	18.85	0.0008
2	0	1	0	4	2		< 0.05
3	1	0	1	6	2		
4	0	1	0	8	1		
5	0	0	0	6	2		
6	1	1	1	9	0		
mean ± SD	0.5 ± 0.54	0.5 ± 0.54	0.33 ± 0.51	6.33 ± 1.86[a]	1.33 ± 0.81[b]		

(n = 6)
[a] : highly significant difference as compared to the control group ($p < 0.001$),
[b] : highly significant difference as compared to the Ag NPs group ($p < 0.001$)

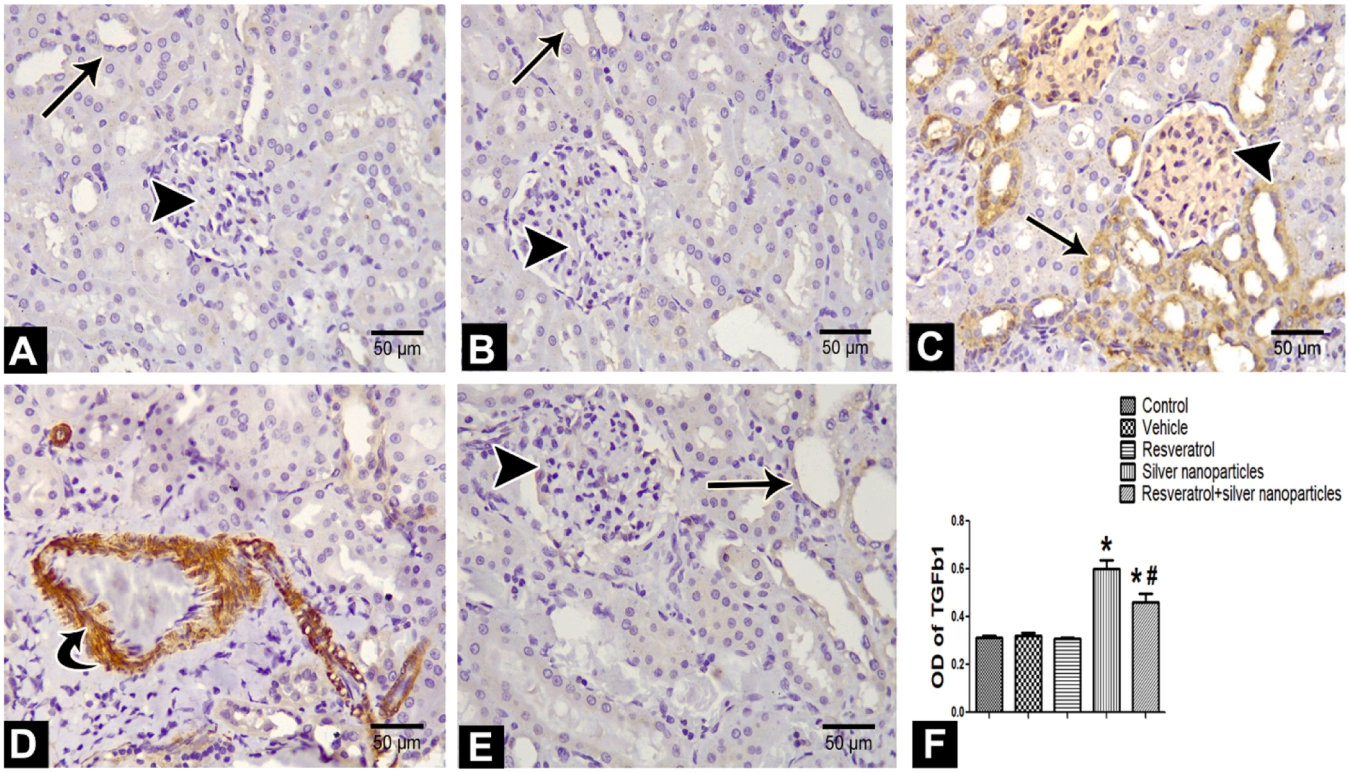

Fig. 12. Photomicrographs of renal cortex sections of different groups; (A, B): The control and resveratrol groups respectively showed negative expression of TGF-β1 in the glomeruli (arrowhead) and epithelial cells of the tubules (arrow). (C, D): The Ag NPs group showed positive cytoplasmic TGF-β1 immunostaining in glomeruli (arrowhead), epithelial cells of distal convoluted tubules (arrow), and strong positive expression in the walls of blood vessels (curved arrow). (E) The resveratrol + Ag NPs group showed mild positive expression in the glomeruli (arrowhead) and epithelial cells of the tubules (arrow). (TGF-β1 immunostaining, X 400, scale bar 50 µm). (F) Effect of Ag NPs on optical density (OD) of TGF-β1 immunoreactions in the renal cortex among different studied groups, and role of resveratrol. Values are presented as the mean ± standard deviation (SD) TGF-β1 immunoreactions. * : $p < 0.05$ compared to control, vehicle and resveratrol groups, #: $p < 0.05$ compared to silver nanoparticles group.

positive expression was observed in the walls of blood vessels. In addition, Ag NPs treated rats (group IV) showed a highly significant increase ($p<0.001$) in the optical density (OD) of TGF-β1 immunoreactions when compared with groups I, II, and III, Fig. 12C, D, F. While group V (resveratrol + Ag NPs) exposed minimal cytoplasmic brown stains with a highly significant decrease in OD of TGF-β1 ($p<0.001$) relative to Ag NPs group (group IV). Fig. 12D, E, F.

Regarding claudin-1 immune-marker expression, groups I and III (control & resveratrol groups) showed negative expression of claudin-1 staining in the epithelial cells of convoluted tubules as well as of the glomeruli, Fig. 13A, B. Group IV (Ag NPs group) revealed strong positive claudin-1immunostaining in the form of brown cytoplasmic stains in glomeruli in addition to epithelial cells of distal convoluted tubules. Group IV demonstrated a highly significant increase in OD of claudin 1 in comparison with groups I, II, and III ($p<0.001$), Fig. 13 C, E. While, group V (resveratrol + Ag NPs) exposed moderate brown cytoplasmic stains with a significant reduction in OD of claudin 1 compared to group IV ($p<0.05$), Fig. 13D, E.

5. Discussion

As a part of our daily lives, exposure to nanoparticles has become unavoidable [71]. Extensive uses of Ag NPs in different industries as medicine, food, and agriculture, make the researchers and others focus on studying their potential health hazards on various biological systems [67,95,96]

This study was carried out to examine the possible renal toxic outcomes of exposure to Ag NPs on adult male albino rats and the possible underlying mechanisms with the evaluation of resveratrol in amelioration or protection against such effects.

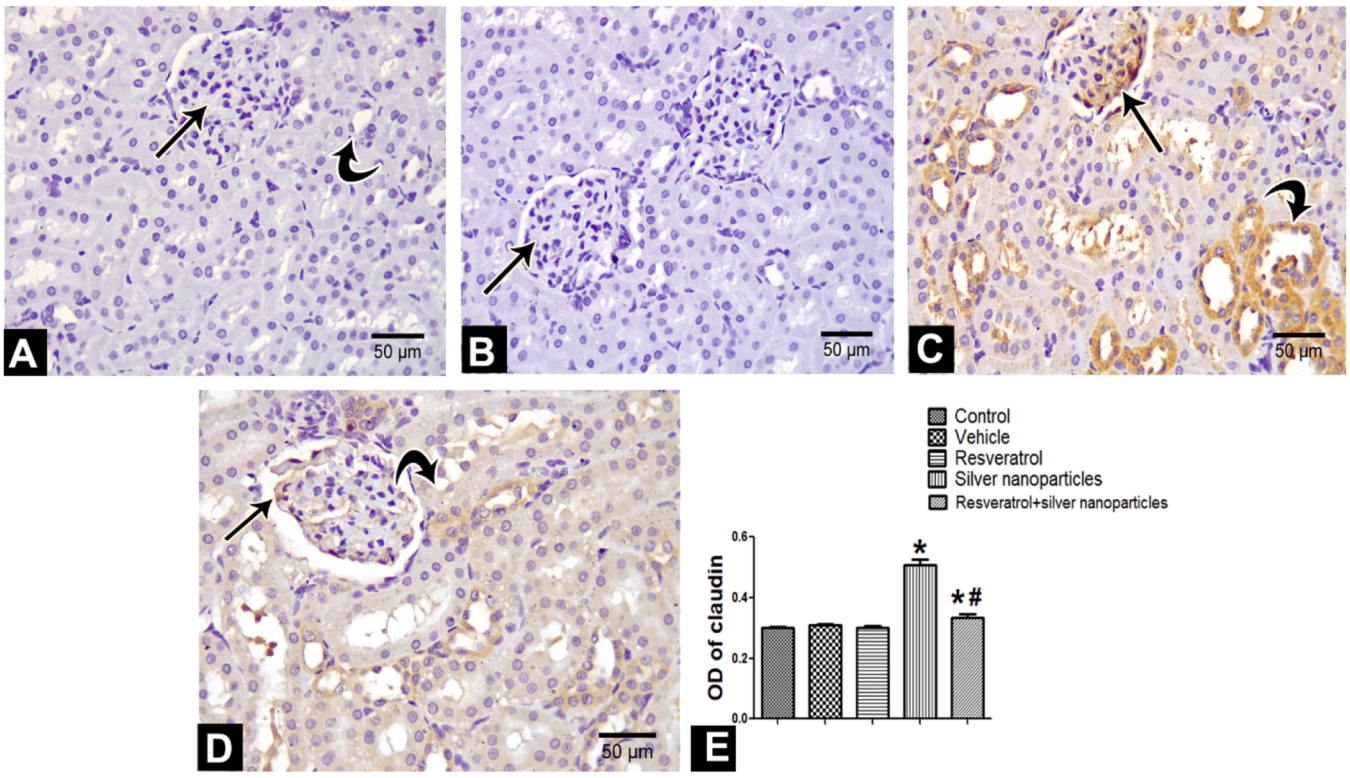

Fig. 13. Photomicrographs of renal cortex sections of different groups; (A, B): The control and resveratrol groups respectively showed negative expression of claudin-1 in the glomeruli (arrow) and epithelial cells of the convoluted tubules (curved arrow). (C): The Ag NPs group showed positive cytoplasmic claudin-1 immunostaining in glomeruli (arrow), epithelial cells of distal convoluted tubules (curved arrow). (D) The resveratrol + Ag NPs group showed moderate positive expression in the glomeruli (arrow) and epithelial cells of the tubules (curved arrow) (Claudin 1 immunostaining, X 400, scale bar 50 µm) (E). Effect of Ag NPs on optical density (OD) of claudin1 immunoreactions in the renal cortex among different studied groups, and role of resveratrol. Values are presented as the mean ± standard deviation (SD) Claudin 1 immunoreactions. * : $p < 0.05$ compared to control, vehicle and resveratrol groups, #: $p < 0.05$ compared to silver nanoparticles group.

The results of this scientific research revealed a reduction in absolute and relative kidney weight in rats taking Ag NPs for 4 weeks. These are compatible with the results of [88] who found a reduction in kidney weight after 60 days of Ag NPs treatment, unlike [62] who found non-significant alterations in the reno-somatic index during the 28-day study.

Concerning *blood and urinary renal injury* biomarkers, Ag NPs usage caused obvious increases in serum levels of creatinine and urea which are in agreement with several studies that showed adverse renal insult of Ag NPs [30,36,59,62,78,99].

Administration of Ag NPs for 4 weeks caused a rise in serum levels of potassium and a decrease in serum levels of sodium, in addition to increases in urinary levels of KIM-1, NGAL, and cystatin C in this experimental study. Beltagy et al., [10] displayed an increase in potassium levels with a decrease in sodium levels after treatment of rats with Magnetite silver nanoparticles for 4 weeks. Damaged tubular cells may be the cause of hyperkalemia and hyponatremia as occurs in chronic renal failure [82].

Searching for new early and sensitive biomarkers for kidney injury instead of routine serum creatinine is on the rise due to many reasons including the influence of serum creatinine by non-renal factors such as age, gender, dietary habits, muscular mass, and hydration status [52]. Also, serum creatinine may not rise except after loss of more than half the renal function, so, it doesn't give an actual estimation of glomerular filtration [22].

NGAL, KIM-1, and cystatin-C are new promising early renal biomarkers [70]. Urinary NGAL and KIM-1 were increased in synchronization with the increased ratio of urine albumin-to-creatinine, making them significant predictors of albuminuria [104]. Cystatin C is used to assess glomerular filtration rate and predict renal dysfunction progression better than serum creatinine [40].

In this study, Ag NPs administration caused increases in oxidative stress markers involving protein carbonyl, myeloperoxidase activity, MDA, and xanthine oxidase with a reduction in antioxidant markers including superoxide dismutase and catalase activity in renal tissues. Moreover, it decreased serum SIRT1 levels and induced upregulation of IL1-β, TNF-α, and MCP-1gene expressions with downregulation of nephrin and podocin gene expressions in renal tissues. Administration of resveratrol with Ag NPs resulted in partial improvement of all biochemical parameters.

We observed negative correlations between podocin, nephrin, oxidative stress markers, and pro-inflammatory cytokines (IL1-β, TNF-α). However positive correlations between podocin, nephrin, superoxide dismutase, catalase, and with SIRT1 levels. The opposite of the previous results was observed when correlated between the result of MCP-1 and the results of the above parameters.

Our results are in parallel to many studies demonstrating the ability of Ag NPs to increase oxidative stress markers with a decline in antioxidant markers [30,3,50,59,78].

After Ag NPs come into the cell via endocytosis, they are moved to the lysosome. The acidic milieu of the lysosome causes dissolution and liberation of silver ions, and then degradation of the cell with the liberation of nanosilver occurs releasing a high amount of reactive oxygen species (ROS) and causing a higher grade of cytotoxicity [61,93,102]. According to [80] study, the NADPH oxidase (NOX) family, especially NOX4, is the main origin of renal ROS. A correlation and matchmaking between NOX4 up-regulation and ROS production was found in a study done by [51], supporting the point that NOX4 is the main source of Ag NPs -induced toxicity.

Adult podocytes lack the ability of self-renewal, with oxidative

stress, inflammatory processes, apoptosis, and autophagy resulting in a reduction in nephrin and podocin proteins essential for maintaining podocyte's structure and functions with subsequent development and/or progression of glomerular diseases [47].

Several in vitro studies displayed that oxidative stress induced by different insults can cause podocyte damage [103,56]. In cultured podocytes, induction of NOX4 expression by high glucose and TGF-β1 increased ROS production causing a variety of lesions including podocyte apoptosis, inflammation, and fibrosis [14,37].

Many studies have established that Ca^{2+} homeostatic proteins are sensitive to oxidative stress, making them important targets of ROS [89]. A widely expressed channel in different kidney cells including podocytes is Ca^{2+}-permeable transient receptor potential cation channel 6 (TRPC6) [25] whose failure is neatly related to proteinuria [19]. Regression and damage of podocyte foot processes caused by overexpression of TRPC6 affect glomerular filtration [98]. A study by [51] displayed an overexpression of TRPC6 after 3 weeks of Ag NPs exposure which was matched with the urinary microalbumin present in that study.

There is a link between oxidative stress and the inflammation pathway. It was reported that the production of inflammatory cytokines like IL-1β and TNF-α can be triggered by excess ROS through activating mediator signaling molecules [60]. This is supported by the study of [51] who found that TNF-α and IL-1β expression in renal tissues upregulated after 2–3 weeks of Ag NPs exposure emphasizing the relation between proinflammatory cytokines and ROS and proposed that oxidative stress has a role in nephrotoxicity caused by Ag NPs. Moreover, increased levels of renal inflammatory cytokines IL-1β, TNF-α associated with excess ROS were observed after exposure to Ag NPs in the kidney by previous studies [78,81].

One of the possible mechanisms of proteinuric glomerulopathies is glomerular inflammation. Podocytes can contribute to glomerular inflammation by releasing inflammatory cytokines when injured and also, they express receptors for different inflammatory cytokines (e.g., TNF-α and IL-1β) putting them as potential targets of the baleful effects of these inflammatory cytokines [68,8].

Different cell types in the kidney secrete the MCP-1 including podocytes. Activation of glomerular monocyte occurs in response to the joining of MCP-1 to the cognate receptor, C–C chemokine receptor 2 (CCR2) [8]. MCP-1 can harm podocytes by attracting macrophages, and by direct influence on podocytes that express CCR2 and it has overexpressed in several proteinuric diseases. In addition, *in* vitro research has shown the joining of MCP-1 to CCR2 can down-regulate nephrin, podocyte peregrination, and apoptosis [7].

SIRT 1 is the main member of the sirtuin family which is a group of nicotinamide adenine dinucleotide (NAD+)-dependent deacetylases involved in the regulation of histones deacetylation in the promoter regions of the downstream gene. Alteration of this process results in many injurious effects including podocytopathy, apoptosis, autophagic cell death, inflammatory responses, disruption of cell-cell adhesion, and release of reactive oxygen radicals [18].

Chuang et al., [11] and [31] have revealed that SIRT1 has a protective function against podocyte injury. This is in line with that finding detected by [58] and [38] who noticed marked exacerbation of podocyte damage in podocyte Sirt1 knockout mice.

Consistent with our results, Wang et al. [94] stated clinical proof proved that the downregulation of SIRT1 was associated with inflammatory processes which have been ameliorated (attenuated) by resveratrol through pharmacological activation of SIRT 1.

In the current study, the histopathological changes of the kidney ensure the biochemical findings of treated animals. The treated animals showed glomerular and tubular alterations and distortion with marked atrophy of the glomerulus and widening of the Bowman's space. Also, there was flatting of tubular lining epithelium that showed degeneration with pyknotic nuclei and sloughing of cells from their basement membrane into their lumen. These changes were in agreement with [62] who reported the same changes in the kidney treated with Ag NPs for repeated 28 days. They explained these histopathological changes due to the accumulation & deposition of Ag NPs along the mesangium and glomerular basement membrane, as kidneys are one of the most susceptible organs after long nanoparticle exposure [39].

Atrophic changes with the widening of Bowman's spaces were attributed to periglomerular fibrosis and thickening of the glomerular basement membrane leading to disturbance in glomerular outflow and cystic changes in Bowman's space [85]. Confirming the deleterious effects of toxic nanoparticles, evaluations of different kinds of nanoparticles have shown the same results [1,53,76].

Vascular congestion and cellular infiltration detected in this study were consistent with other studies which reported that different nanoparticles resulted in congestion and expansion of renal tubular capillaries with infiltration of inflammatory cells [34,65]. The authors related these vascular changes to the oxidative stress effect of Ag NPs, the defense mechanism against an injurious toxin, and the increase in the cell membrane permeability, leading to intracellular accumulation of water [74,90].

The current study showed marked collagen deposition inside the glomeruli, peritubular, and interstitial tissue around blood vessels between renal tubules in the silver nanoparticles group (IV) compared to other groups. This was confirmed morphometrically as the mean area percentage of collagen fibers in group IV was significantly higher than that of the other groups. These findings are in accordance with the results of [62].

The excessive accumulation of collagen fibrils is associated with interstitial tissue fibrosis which is a common feature of various diseases that causes chronic renal failure [9].

A variety of inflammatory cells and growth factors, such as TGF-β1, participated in renal interstitial fibrosis. TGF-β1 is thought to be a key mediator in this fibrosis process [23]. This explained the increased expression of TGF-β1 in group IV (silver nanoparticles) which revealed strong positive cytoplasmic TGF-β1 immunostaining in the form of brown stains distributed in the cytoplasm of glomerular and epithelial cells of distal convoluted tubules, also in the walls of blood vessels. This was confirmed morphometrically where there was a highly significant increase in the optical density (OD) of TGF-β1 immunoreactions in group IV when compared with other groups. These results are consistent with the results of [62] who found an increase in the expression of TGF-β1 three times in the group treated with 125 mg/kg of Ag NPs more than the control group.

The positive relationship between the appearance of TGF-β1 and the severity of renal dysfunction associated with tubulointerstitial injury has been stated also in many studies, which reported that TGF-β1 contributes to tubulointerstitial damage and renal dysfunction by inducing apoptosis and increasing fibrosis leading to tubular epithelial cell loss [5,87].

SIRT1 is an antifibrotic factor that was recorded by previous studies on different organs [13,42]. In renal tissues, SIRT1 can reduce renal fibrosis by inhibiting TGF- β1 signaling through deacetylating Smad3, and this effect was partially protected by the addition of resveratrol [32,101]. This point is consistent with our results in which treatment with Ag NPs reduced SIRT1 levels with increased expression in TGF- β1, and resveratrol protected against such changes.

Claudin is a fundamental component of tight junction complexes in epithelial, endothelial cells, and podocytes [43,45,92]. Claudin-1 is one of the claudin subtypes that is expressed in the tight junctions of parietal epithelial cells of Bowman's capsule in both human patients with glomerulonephritis and murine models, so it is considered a marker of parietal epithelial cells of Bowman's capsule [41,83].

In the present study, Group IV (silver nanoparticles group) revealed strong positive claudin-1immunostaining in the form of brown cytoplasmic stains in glomeruli in addition to epithelial cells of distal convoluted tubules. This was confirmed morphometrically in which there was a significant increase in OD of claudin 1 in group IV in comparison with other groups with partial protection provided by resveratrol as

shown in group V. These results are in accordance with those of [41,44], who discovered claudin-1 immunohistochemistry expression in crescentic lesions of the human renal cortex, which include the collecting duct, distal convoluted tubule, and parietal epithelium of Bowman's capsule.

Also, SIRT1 acts as an important regulator of podocyte function and can modify the tight junction claudin-1 expression in podocytes. It was noticed that diabetes downregulates SIRT1 in proximal tubules resulting in increased claudin-1 expression in podocytes leading to an increment in glomerular permeability with albuminuria [29]. This is consistent with our results as Ag NPs in group (IV) reduced SIRT1 levels with increased claudin-1 expression, and resveratrol protected against such changes.

Moreover, a recent study suggested that the inflammatory cells and fibrosis around the glomeruli and renal tubules cause an increase in claudin-1 expression [35]. This was strengthened by the study of [4] who proved that TNF-α increases claudin-1 expression in the pig tubular cell. This is following our results where there was significant upregulation of the TNF-α gene and claudin-1 immuno-expression in the Ag NPs group (IV) compared to other groups, but, administration of resveratrol with Ag NPs in the group (V) protected these upregulations.

The above-mentioned biochemical, histopathological, and immunohistochemical results in the treated group (IV) exhibited obvious improvement with the administration of resveratrol+Ag NPs in group (V). This renoprotective effect of resveratrol was related to its inhibition of the production of reactive oxygen and reactive nitrogen species, restoration of endogenous antioxidants (SOD, CAT, and glutathione peroxidase), and improvement of vascular function by increasing nitric oxide synthesis and inhibition of its degradation [64,79]. Also, de Sá Coutinho et al. [17] stated that resveratrol has potent anti-inflammatory activity in renal mesangial cells through modification of the p38 mitogen-activated protein kinase signaling pathway

Pan et al., [64] observed a significant reversal of proteinuria, associated with recuperation expression of nephrin and podocin protein with repression of renal NF-κB activity, TNF-α, and MCP-1 level after resveratrol usage. Moreover, [33,51] assumed the renoprotective effect of resveratrol with alleviation of podocyte injury due to stimulation of autophagy together with suppression of NF-κB signaling pathway and oxidative stress processes.

Moreover, these results are matched with the results of [26] who proved that resveratrol application significantly ameliorates hypertension-induced morphological changes in the kidney.

6. Conclusion

Renal toxicity caused by Ag NPs was demonstrated by elevated levels of NGAL, KIM-1, cystatin, creatinine, urea, and potassium. Increased oxidative stress markers (protein carbonyl, MDA, myeloperoxidase activity) and decreased antioxidant markers (SOD, catalase) in renal tissues were the mediating factors for these detrimental effects. Furthermore, it was noted that inflammatory markers (TNF-α and IL1-β) were upregulated. These were linked to the downregulation of nephrin and podocin, as well as overexpression of MCP-1 expressions in renal tissues, and reductions in serum levels of SIRT1. The glomerular and tubular alterations, distortion with marked atrophy of the glomerulus, widening of the Bowman's space, flatting of the tubular lining epithelium with pyknotic nuclei, and sloughing of cells from their basement membrane; all of which were histopathologically detected in renal tissues supported these toxic changes, in addition to a noticeable rise in TGF-β1 and Claudin-1 immune expression. Resveratrol's antioxidant, anti-inflammatory, and SIRT1-activating properties offered protection against the aforementioned alterations.

Ethical approval

Under the number ZU-IACUC/3/F/157/2022, the Institutional Animal Care and Use of Zagazig University, Egypt approved this experimental protocol in accordance with applicable international laws and regulations encouraging the researchers to achieve their duties to perform animal experiments with the highest level of scientific, humane, and ethical rules [12].

Authors Statement

The authors declare that they have no known competing financial interests or personal relationships that could have appeared to influence the work reported in this paper.

Consent to publish

all authors agree to publish this article in this journal

Consent to participate

all authors participate in this study

Funding

There is no fund is this study.

CRediT authorship contribution statement

Eman El-Sayed Khayal: Writing – review & editing, Writing – original draft, Methodology, Investigation. **Mona G. Elhadidy:** Writing – original draft, Methodology, Data curation, Conceptualization. **Sulaiman Mohammed Alnasser:** Supervision, Data curation. **Manal Mohammad Morsy:** Writing – review & editing, Writing – original draft, Supervision. **Azza I. Farag:** Writing – review & editing, Writing – original draft. **Samah A. El-Nagdy:** Writing – review & editing, Writing – original draft.

Declaration of Competing Interest

The authors declare that they have no known competing financial interests or personal relationships that could have appeared to influence the work reported in this paper.

Data availability

No data was used for the research described in the article.

References

[1] M.A.K. Abdelhalim, B.M. Jarrar, Renal tissue alterations were size-dependent with smaller ones induced more effects and related with time exposure of gold nanoparticles, Lipids Health Dis. 10 (2011) 163.
[2] H. Aebi, Catalase in vitro, Methods Enzym. 105 (1984) 121–126.
[3] M.K. Alatawi, A.A. Alasmari, A.D. Alaliany, M.M. Almajed, M.I. Sakran, Silver nanoparticles forensic uses and toxicity on vital organs and different body systems, Adv. Toxicol. Toxic. Eff. 8 (2024) 015–029.
[4] Y. Amoozadeh, Q. Dan, S. Anwer, H.H. Huang, V. Barbieri, F. Waheed, M. Maishan, K. Szászi, Tumor Necrosis Factor-α Increases Claudin-1, 4, and 7 Expression in Tubular Cells: Role in Permeability Changes, J. Cell Physiol. 232 (2017) 2210–2220.
[5] P. August, M. Suthanthiran, Transforming growth factor beta and progression of renal disease: Management of comorbidities in kidney disease in the 21st century: Anemia and bone disease, Kidney Int. 64 (2003) S99–S104.
[6] J.D. Bancroft, M. Gamble, Theory and Practice of Histological Techniques, Elsevier health sciences, 2008.
[7] F. Barutta, S. Bellini, G. Gruden, Mechanisms of podocyte injury and implications for diabetic nephropathy, Clin Sci (Lond) 136 (7) (2022) 493–520, https://doi.org/10.1042/CS20210625.
[8] F. Barutta, G. Bruno, S. Grimaldi, G. Gruden, Inflammation in diabetic nephropathy: moving toward clinical biomarkers and targets for treatment, Endocrine 48 (2015) 730–742.
[9] S. Bedi, A. Vidyasagar, A. Djamali, Epithelial-to-mesenchymal transition and chronic allograft tubulointerstitial fibrosis, Transpl. Rev. (Orlando) 22 (2008) 1–5.

[10] D. Beltagy, E. Tousson, N. Abdo, B. Izzularab, Protective role of chichorium intybus extract against renal toxicity induced by magnetite silver nanoparticles in male rats, OnLine J. Biol. Sci. 21 (2021) 251–260.

[11] P.Y. Chuang, W. Cai, X. Li, L. Fang, J. Xu, R. Yacoub, J.C. He, K. Lee, Reduction in podocyte SIRT1 accelerates kidney injury in aging mice, Am. J. Physiol. Ren. Physiol. 313 (2017) F621–F628.

[12] J.D. Clark, G.F. Gebhart, J.C. Gonder, M.E. Keeling, D.F. Kohn, The 1996 guide for the care and use of laboratory animals, ILAR J. 38 (1997) 41–48.

[13] S. Costa Cdos, T.O. Hammes, F. Rohden, R. Margis, J.W. Bortolotto, A.V. Padoin, C.C. Mottin, R.M. Guaragna, SIRT1 transcription is decreased in visceral adipose tissue of morbidly obese patients with severe hepatic steatosis, Obes. Surg. 20 (2010) 633–639.

[14] R. Das, S. Xu, X. Quan, T.T. Nguyen, I.D. Kong, C.H. Chung, E.Y. Lee, S.K. Cha, K. S. Park, Upregulation of mitochondrial Nox4 mediates TGF-β-induced apoptosis in cultured mouse podocytes, Am. J. Physiol. Ren. Physiol. 306 (2014) F155–F167.

[15] V. De Matteis, Exposure to inorganic nanoparticles: routes of entry, immune response, biodistribution and in vitro/in vivo toxicity evaluation, Toxics 5 (2017).

[16] A.C.N. De Moraes, C.B.V. De Andrade, I.P.R. Ramos, M.L. Dias, C.M.P. Batista, C. F. Pimentel, J.J. De Carvalho, R. Goldenberg, Resveratrol promotes liver regeneration in drug-induced liver disease in mice, Food Res Int 142 (2021) 110185.

[17] D. de Sá Coutinho, M.T. Pacheco, R. Luiz Frozza, A. Bernardi, Anti-Inflammatory Effects of Resveratrol: Mechanistic Insights, Int J Mol Sci 19 (6) (2018) 1812, https://doi.org/10.3390/ijms19061812. Jun 20.

[18] Z. Deng, Y. Li, H. Liu, S. Xiao, L. Li, J. Tian, C. Cheng, G. Zhang, F. Zhang, The role of sirtuin 1 and its activator, resveratrol in osteoarthritis, Biosci. Rep. 39 (2019).

[19] Dietrich, A., Chubanov, V. & Gudermann, T.J.J.O.T.A.S.O.N.J. 2010. Renal TRPathies. 21 5, 736-744.

[20] Y.J. Dong, N. Liu, Z. Xiao, T. Sun, S.H. Wu, W.X. Sun, Z.G. Xu, H. Yuan, Renal protective effect of sirtuin 1, J. Diabetes Res 2014 (2014) 843786.

[21] T. Elmasry, N. Al-Shaalan, E. Tousson, K. Elmorshedy, A. Al-Ghadeer, P53 expression in response to equigan induced testicular injury and oxidative stress in male rat and the possible prophylactic effect of star anise extracts, Annu. Res. Rev. Biol. 14 (2017) 1–8.

[22] A. Farrar, Acute kidney injury, Nurs. Clin. North Am. 53 (2018) 499–510.

[23] A.B. Farris, R.B. Colvin, Renal interstitial fibrosis: mechanisms and evaluation, Curr. Opin. Nephrol. Hypertens. 21 (2012) 289–300.

[24] Gelen, V. & Sengul, E. 2021. Protective effects of resveratrol on kidney function tests and renal histopathology in carbon tetrachloride-induced renal toxicity in rats. 10, 156-161.

[25] M. Goel, W.G. Sinkins, C.D. Zuo, M. Estacion, W.P. Schilling, Identification and localization of TRPC channels in the rat kidney, Am. J. Physiol. Ren. Physiol. 290 (2006) F1241–F1252.

[26] J. Grujić-Milanović, V. Jaćević, Z. Miloradović, S.D. Milanović, D. Jovović, M. Ivanov, D. Karanović, U.-J. Vajić, N. Mihailović-Stanojević, Resveratrol improved kidney function and structure in malignantly hypertensive rats by restoration of antioxidant capacity and nitric oxide bioavailability, Biomed. Pharmacother. 154 (2022) 113642.

[27] S.R. Hamad, Cardio-renal protective role of cerium oxide nanoparticle in preventing histopathological lesions, and collagen deposition produced from lead acetate injection in vivo: light microscopic examination %, J. Egypt. J. Histol. 45 (2022) 815–824.

[28] Q. Hao, X. Xiao, J. Zhen, J. Feng, C. Song, B. Jiang, Z. Hu, Resveratrol attenuates acute kidney injury by inhibiting death receptor-mediated apoptotic pathways in a cisplatin-induced rat model, Mol. Med Rep. 14 (2016) 3683–3689.

[29] K. Hasegawa, S. Wakino, P. Simic, Y. Sakamaki, H. Minakuchi, K. Fujimura, K. Hosoya, M. Komatsu, Y. Kaneko, T. Kanda, E. Kubota, H. Tokuyama, K. Hayashi, L. Guarente, H. Itoh, Renal tubular Sirt1 attenuates diabetic albuminuria by epigenetically suppressing Claudin-1 overexpression in podocytes, Nat. Med 19 (2013) 1496–1504.

[30] Hassan, O.A., Saad, A.H., Hamouda, A.A.H.J.T.E.J.O.F.S. & Toxicology, A. 2019. Silver nanoparticles induced multiple organ toxicity in mice. 19, 31-47.

[31] Q. Hong, L. Zhang, B. Das, Z. Li, B. Liu, G. Cai, X. Chen, P.Y. Chuang, J.C. He, K. Lee, Increased podocyte Sirtuin-1 function attenuates diabetic kidney injury, Kidney Int 93 (2018) 1330–1343.

[32] X.Z. Huang, D. Wen, M. Zhang, Q. Xie, L. Ma, Y. Guan, Y. Ren, J. Chen, C.M. Hao, Sirt1 activation ameliorates renal fibrosis by inhibiting the TGF-β/Smad3 pathway, J. Cell Biochem 115 (2014) 996–1005.

[33] H. Huang, Y. You, X. Lin, C. Tang, X. Gu, M. Huang, Y. Qin, J. Tan, F. Huang, Inhibition of TRPC6 signal pathway alleviates podocyte injury induced by TGF-β1, Cell Physiol. Biochem 41 (2017) 163–172.

[34] K.E. Ibrahim, M.G. Al-Mutary, A.O. Bakhiet, H.A. Khan, Histopathology of the liver, kidney, and spleen of mice exposed to gold nanoparticles, Molecules 23 (2018).

[35] M. Iida, S. Ohtomo, N.A. Wada, O. Ueda, Y. Tsuboi, A. Kurata, K.I. Jishage, N. Horiba, TNF-α induces Claudin-1 expression in renal tubules in Alport mice, PLoS One 17 (2022) e0265081.

[36] Ismail, H.K., Alkshab, A., Al-Baker, A.J.I.J.O.F.M. & Toxicology 2020. Effect of orally-administered silver nanoparticles (Ag-NPs) on some biochemical parameters in kidney of rats. 14, 1732-1738.

[37] J.C. Jha, S.P. Gray, D. Barit, J. Okabe, A. El-Osta, T. Namikoshi, V. Thallas-Bonke, K. Wingler, C. Szyndralewiez, F. Heitz, R.M. Touyz, M.E. Cooper, H.H. Schmidt, K.A. Jandeleit-Dahm, Genetic targeting or pharmacologic inhibition of NADPH oxidase nox4 provides renoprotection in long-term diabetic nephropathy, J. Am. Soc. Nephrol. 25 (2014) 1237–1254.

[38] M. Jiang, M. Zhao, M. Bai, J. Lei, Y. Yuan, S. Huang, Y. Zhang, G. Ding, Z. Jia, A. Zhang, SIRT1 alleviates aldosterone-induced podocyte injury by suppressing mitochondrial dysfunction and NLRP3 inflammasome activation, Kidney Dis. (Basel) 7 (2021) 293–305.

[39] Y.S. Kim, J.S. Kim, H.S. Cho, D.S. Rha, J.M. Kim, J.D. Park, B.S. Choi, R. Lim, H. K. Chang, Y.H. Chung, I.H. Kwon, J. Jeong, B.S. Han, I.J. Yu, Twenty-eight-day oral toxicity, genotoxicity, and gender-related tissue distribution of silver nanoparticles in Sprague-Dawley rats, Inhal. Toxicol. 20 (2008) 575–583.

[40] S.S. Kim, S.H. Song, I.J. Kim, Y.K. Jeon, B.H. Kim, I.S. Kwak, E.K. Lee, Y.K. Kim, Urinary cystatin C and tubular proteinuria predict progression of diabetic nephropathy, Diabetes Care 36 (2013) 656–661.

[41] A. Kirk, S. Campbell, P. Bass, J. Mason, J. Collins, Differential expression of claudin tight junction proteins in the human cortical nephron, Nephrol. Dial. Transpl. 25 (2010) 2107–2119.

[42] M. Kitada, A. Takeda, T. Nagai, H. Ito, K. Kanasaki, D. Koya, Dietary restriction ameliorates diabetic nephropathy through anti-inflammatory effects and regulation of the autophagy via restoration of Sirt1 in diabetic Wistar fatty (fa/fa) rats: a model of type 2 diabetes, Exp. Diabetes Res 2011 (2011) 908185.

[43] Y. Kiuchi-Saishin, S. Gotoh, M. Furuse, A. Takasuga, Y. Tano, S. Tsukita, Differential expression patterns of claudins, tight junction membrane proteins, in mouse nephron segments, J. Am. Soc. Nephrol. 13 (2002) 875–886.

[44] R. Koda, A. Yoshino, Y. Imanishi, S. Kawamoto, Y. Ueda, E. Yaoita, J.J. Kazama, I. Narita, T. Takeda, Expression of tight junction protein claudin-1 in human crescentic glomerulonephritis, Int J. Nephrol. 2014 (2014) 598670.

[45] R. Koda, L. Zhao, E. Yaoita, Y. Yoshida, S. Tsukita, A. Tamura, M. Nameta, Y. Zhang, H. Fujinaka, S. Magdeldin, B. Xu, I. Narita, T. Yamamoto, Novel expression of claudin-5 in glomerular podocytes, Cell Tissue Res 343 (2011) 637–648.

[46] O. Kose, D. Beal, S. Motellier, N. Pelissier, V. Collin-Faure, M. Blosi, R. Bengalli, A. Costa, I. Furxhi, P. Mantecca, M. Carriere, Physicochemical transformations of silver nanoparticles in the oro-gastrointestinal tract mildly affect their toxicity to intestinal cells in vitro: an AOP-oriented testing approach, Toxics 11 (2023).

[47] I. Kravets, S.K. Mallipattu, The role of podocytes and podocyte-associated biomarkers in diagnosis and treatment of diabetic kidney disease, J. Endocr. Soc. 4 (2020) bvaa029.

[48] H. Kruijswijk, Clinical chemistry: Principles and technics, 267 illustrations, $37.50, in: R.J. Henry, D.C. Cannon, J.W. Winkelman (Eds.), 2nd edn.Harper and Row, Hagerstown (Md.), 1974, Elsevier, New York, Evanston, San Francisco, London, 1975, p. 1641.

[49] R.L. Levine, D. Garland, C.N. Oliver, A. Amici, I. Climent, A.G. Lenz, B.W. Ahn, S. Shaltiel, E.R. Stadtman, Determination of carbonyl content in oxidatively modified proteins, Methods Enzym. 186 (1990) 464–478.

[50] B. Li, X. Xiao, Y. Miao, L. Guo, J. Zhen, X. Li, B. Jiang, Z. Hu, Resveratrol alleviates obesity-associated podocyte injury in ovariectomized obese rats, Exp. Ther. Med 19 (2020) 123–130.

[51] Y. Liu, L. Sun, G. Yang, Z. Yang, Nephrotoxicity and genotoxicity of silver nanoparticles in juvenile rats and possible mechanisms of action, Arch. Ind. Hyg. Toxicol. 71 (2020) 121–129.

[52] S. Lopez-Giacoman, M. Madero, Biomarkers in chronic kidney disease, from kidney function to kidney damage, World J. Nephrol. 4 (2015) 57–73.

[53] P. Ma, Q. Luo, J. Chen, Y. Gan, J. Du, S. Ding, Z. Xi, X. Yang, Intraperitoneal injection of magnetic Fe_3O_4-nanoparticle induces hepatic and renal tissue injury via oxidative stress in mice, Int J. Nanomed. 7 (2012) 4809–4818.

[54] S.K. Mallipattu, J.C. He, The podocyte as a direct target for treatment of glomerular disease? Am. J. Physiol. Ren. Physiol. 311 (2016) F46–F51.

[55] S. Marklund, G. Marklund, Involvement of the superoxide anion radical in the autoxidation of pyrogallol and a convenient assay for superoxide dismutase, Eur. J. Biochem 47 (1974) 469–474.

[56] C.B. Marshall, J.W. Pippin, R.D. Krofft, S.J. Shankland, Puromycin aminonucleoside induces oxidant-dependent DNA damage in podocytes in vitro and in vivo, Kidney Int 70 (2006) 1962–1973.

[57] X.H. Miao, C.G. Wang, B.Q. Hu, A. Li, C.B. Chen, W.Q. Song, TGF-beta1 immunohistochemistry and promoter methylation in chronic renal failure rats treated with Uremic Clearance Granules, Folia Histochem Cytobiol. 48 (2010) 284–291.

[58] S. Motonishi, M. Nangaku, T. Wada, Y. Ishimoto, T. Ohse, T. Matsusaka, N. Kubota, A. Shimizu, T. Kadowaki, K. Tobe, R. Inagi, Sirtuin1 maintains actin cytoskeleton by deacetylation of cortactin in injured podocytes, J. Am. Soc. Nephrol. 26 (2015) 1939–1959.

[59] M. Nabeh, Y. Taalab, D. Abd El Wahab, S. Asker, A. Elbedwehy, M. El Harouny, Silver nanotoxicity on kidneys and ovaries of female albino rats, J. Mansoura J. Forensic Med. Clin. Toxicol. 28 (2020) 1–14.

[60] E. Naik, V.M. Dixit, Mitochondrial reactive oxygen species drive proinflammatory cytokine production, J. Exp. Med 208 (2011) 417–420.

[61] P. Nie, Y. Zhao, H. Xu, Synthesis, applications, toxicity and toxicity mechanisms of silver nanoparticles: A review, Ecotoxicol. Environ. Saf. 253 (2023) 114636.

[62] H. Nosrati, M. Hamzepoor, M. Sohrabi, M. Saidijam, M.J. Assari, N. Shabab, Z. Gholami Mahmoudian, Z. Alizadeh, The potential renal toxicity of silver nanoparticles after repeated oral exposure and its underlying mechanisms, BMC Nephrol. 22 (2021) 228.

[63] J. Ott Joslin, Blood collection techniques in exotic small mammals, J. Exot. Pet. Med. 18 (2009) 117–139.

[64] Q.R. Pan, Y.L. Ren, J.J. Zhu, Y.J. Hu, J.S. Zheng, H. Fan, Y. Xu, G. Wang, W.X. Liu, Resveratrol increases nephrin and podocin expression and alleviates renal damage in rats fed a high-fat diet, Nutrients 6 (2014) 2619–2631.
[65] E.J. Park, E. Bae, J. Yi, Y. Kim, K. Choi, S.H. Lee, J. Yoon, B.C. Lee, K. Park, Repeated-dose toxicity and inflammatory responses in mice by oral administration of silver nanoparticles, Environ. Toxicol. Pharm. 30 (2010) 162–168.
[66] D.A. Parks, T.K. Williams, J.S. Beckman, Conversion of xanthine dehydrogenase to oxidase in ischemic rat intestine: a reevaluation, Am. J. Physiol. 254 (1988) G768–G774.
[67] Patel, R.R., Singh, S.K. & Singh, M.J.M.A. 2023. Green synthesis of silver nanoparticles: methods, biological applications, delivery and toxicity. 4, 1831-1849.
[68] C.E. Pedigo, G.M. Ducasa, F. Leclercq, A. Sloan, A. Mitrofanova, T. Hashmi, J. Molina-David, M. Ge, M.I. Lassenius, C. Forsblom, M. Lehto, P.H. Groop, M. Kretzler, S. Eddy, S. Martini, H. Reich, P. Wahl, G. Ghiggeri, C. Faul, G. W. Burke, 3rd, O. Kretz, T.B. Huber, A.J. Mendez, S. Merscher, A. Fornoni, Local TNF causes NFATc1-dependent cholesterol-mediated podocyte injury, J. Clin. Invest 126 (2016) 3336–3350.
[69] L. Pourzahedi, M.J. Eckelman, Environmental life cycle assessment of nanosilver-enabled bandages, Environ. Sci. Technol. 49 (2015) 361–368.
[70] Prasad, R., Choudhary, R., Singh, A., Agarwal, S., Kaushik, P., Singh, K., Yadav, R. R., Yadav, A.S., Bhadauria, D.S. & Lal, H. 2020. Serum Levels of Neutrophil Gelatinase-Associated Lipocalin, Kidney Injury Molecule-1, and Cystatin-C in Renal Artery Stenosis: A Pilot Study. 15, 317-322.
[71] Quevedo, A.C., Lynch, I. & Valsami-Jones, E.J.N. 2021. Silver nanoparticle induced toxicity and cell death mechanisms in embryonic zebrafish cells. 13, 6142-6161.
[72] Rana, S.J.J.T.R.A. 2021. Recent advances on renal toxicity of engineered nanoparticles—A review. 7, 036.
[73] E. Rezvani, A. Rafferty, C. Mcguinness, J. Kennedy, Adverse effects of nanosilver on human health and the environment, Acta Biomater. 94 (2019) 145–159.
[74] E.M. Sadek, N.M. Salama, D.I. Ismail, A.A. Elshafei, Histological study on the protective effect of endogenous stem-cell mobilization in Adriamycin-induced chronic nephropathy in rats, J. Microsc. Ultra 4 (2016) 133–142.
[75] S. Saggu, R. Kumar, Modulatory effect of seabuckthorn leaf extract on oxidative stress parameters in rats during exposure to cold, hypoxia and restraint (C-H-R) stress and post stress recovery, J. Pharm. Pharm. 59 (2007) 1739–1745.
[76] B.D. Sahu, M. Kuncha, G.J. Sindhura, R. Sistla, Hesperidin attenuates cisplatin-induced acute renal injury by decreasing oxidative stress, inflammation and DNA damage, Phytomedicine 20 (2013) 453–460.
[77] Said, N.I., Abd-Elrazek, A.M. & El-Dash, H.A.J.E.T. 2021. The protective role of resveratrol against sulfoxaflor-induced toxicity in testis of adult male rats. 36, 2105-2115.
[78] B. Salama, K.J. Alzahrani, K.S. Alghamdi, O. Al-Amer, K.E. Hassan, M.A. Elhefny, A.J.A. Albarakati, F. Alharthi, H.A. Althagafi, H. Al Sberi, H.K. Amin, M. S. Lokman, K.F. Alsharif, A. Albrakati, A.E. Abdel Moneim, R.B. Kassab, A. S. Fathalla, Silver nanoparticles enhance oxidative stress, inflammation, and apoptosis in liver and kidney tissues: potential protective role of thymoquinone, Biol. Trace Elem. Res 201 (2023) 2942–2954.
[79] J.F. Saldanha, V.O. Leal, F. Rizzetto, G.H. Grimmer, M. Ribeiro-Alves, J. B. Daleprane, J.C. Carraro-Eduardo, D. Mafra, Effects of resveratrol supplementation in Nrf2 and NF-κB expressions in nondialyzed chronic kidney disease patients: a randomized, double-blind, placebo-controlled, crossover clinical trial, J. Ren. Nutr. 26 (2016) 401–406.
[80] Sedeek, M., Nasrallah, R., Touyz, R.M. & Hebert, R.L. 2013. NADPH Oxidases, Reactive Oxygen Species, and the Kidney: Friend and Foe. 24, 1512-1518.
[81] A.M. Shehata, F.M.S. Salem, E.M. El-Saied, S.S. Abd El-Rahman, M.Y. Mahmoud, P.A. Noshy, Evaluation of the ameliorative effect of zinc nanoparticles against silver nanoparticle-induced toxicity in liver and kidney of rats, Biol. Trace Elem. Res 200 (2022) 1201–1211.
[82] Singh, P., Mitra, P., Chambial, S. & Sharma, P. 2017. Study of serum sodium and serum potassium level in chronic renal failurE.
[83] B. Smeets, S. Uhlig, A. Fuss, F. Mooren, J.F. Wetzels, J. Floege, M.J. Moeller, Tracing the origin of glomerular extracapillary lesions from parietal epithelial cells, J. Am. Soc. Nephrol. 20 (2009) 2604–2615.
[84] A. Tabacco, F. Meiattini, E. Moda, P. Tarli, Simplified enzymic/colorimetric serum urea nitrogen determination, Clin. Chem. 25 (1979) 336–337.
[85] M. Takahashi, T. Morita, M. Sawada, T. Uemura, A. Haruna, A. Shimada, Glomerulocystic kidney in a domestic dog, J. Comp. Pathol. 133 (2005) 205–208.
[86] F.W.K. Tam, A.C.M. Ong, Renal monocyte chemoattractant protein-1: an emerging universal biomarker and therapeutic target for kidney diseases? Nephrol. Dial. Transpl. 35 (2020) 198–203.
[87] S.A. Teteris, S.A. Menahem, G. Perry, J.A. Maguire, J.P. Dowling, R.G. Langham, N.M. Thomson, A.N. Stein, Dysregulated growth factor gene expression is associated with tubulointerstitial apoptosis and renal dysfunction, Kidney Int 71 (2007) 1044–1053.
[88] R. Tiwari, R.D. Singh, H. Khan, S. Gangopadhyay, S. Mittal, V. Singh, N. Arjaria, J. Shankar, S.K. Roy, D. Singh, V. Srivastava, Oral subchronic exposure to silver nanoparticles causes renal damage through apoptotic impairment and necrotic cell death, Nanotoxicology 11 (2017) 671–686.
[89] M. Trebak, R. Ginnan, H.A. Singer, D. Jourd'heuil, Interplay between calcium and reactive oxygen/nitrogen species: an essential paradigm for vascular smooth muscle signaling, Antioxid. Redox Signal 12 (2010) 657–674.
[90] A. Troudi, A. Mahjoubi Samet, N. Zeghal, Hepatotoxicity induced by gibberellic acid in adult rats and their progeny, Exp. Toxicol. Pathol. 62 (2010) 637–642.
[91] M.A. Trush, P.A. Egner, T.W. Kensler, Myeloperoxidase as a biomarker of skin irritation and inflammation, Food Chem. Toxicol. 32 (1994) 143–147.
[92] S. Tsukita, Y. Yamazaki, T. Katsuno, A. Tamura, S. Tsukita, Tight junction-based epithelial microenvironment and cell proliferation, Oncogene 27 (2008) 6930–6938.
[93] Waktole, G.J.J.O.B. & Nanobiotechnology 2023. Toxicity and molecular mechanisms of actions of silver nanoparticles. 14, 53-70.
[94] X. Wang, M. Liu, M.J. Zhu, L. Shi, L. Liu, Y.L. Zhao, et al., Resveratrol Protects the Integrity of Alveolar Epithelial Barrier Via Sirt1/Pten/P-Akt Pathway in Methamphetamine-Induced Chronic Lung Injury, Cell Prolif 53 (3) (2020) e12773, https://doi.org/10.1111/cpr.12773.
[95] L. Wen, M. Li, X. Lin, Y. Li, H. Song, H. Chen, AgNPs aggravated hepatic steatosis, inflammation, oxidative stress, and epigenetic changes in mice with NAFLD induced by HFD, Front Bioeng. Biotechnol. 10 (2022) 912178.
[96] L. Xu, Y.Y. Wang, J. Huang, C.Y. Chen, Z.X. Wang, H. Xie, Silver nanoparticles: Synthesis, medical applications and biosafety, Theranostics 10 (2020) 8996–9031.
[97] A. Yahya, W. Adil Obaid, O. Mohammed Hameed, A.F. Hasan, Histopathological and immunohistochemical studies on the effects of silver oxide nanoparticles (AgNPs) on male rats' liver, J. Biosci. Appl. Res. 10 (2024) 392–398.
[98] S. Yu, L. Yu, Dexamethasone Resisted Podocyte Injury via Stabilizing TRPC6 Expression and Distribution, Evid. Based Complement Altern. Med 2012 (2012) 652059.
[99] Zamil, R.Y. A.R. J.A. S.R. J.F. E., Technology, & Sciences, 2018. The Effects of Different Concentrations of Sliver Nanoparticles on the Kidneys of Male Albino Mice. 50, 190-203..
[100] S. Zargar, M. Alonazi, H. Rizwana, T.A. Wani, Resveratrol reverses thioacetamide-induced renal assault with respect to oxidative stress, renal function, DNA damage, and cytokine release in wistar rats, Oxid. Med Cell Longev. 2019 (2019) 1702959.
[101] Y. Zhang, K.A. Connelly, K. Thai, X. Wu, A. Kapus, D. Kepecs, R.E. Gilbert, Sirtuin 1 activation reduces transforming growth factor-β1-induced fibrogenesis and affords organ protection in a model of progressive, experimental kidney and associated cardiac disease, Am. J. Pathol. 187 (2017) 80–90.
[102] J. Zhang, F. Wang, S.S.K. Yalamarty, N. Filipczak, Y. Jin, X. Li, Nano silver-induced toxicity and associated mechanisms, Int J. Nanomed. 17 (2022) 1851–1864.
[103] L.L. Zhou, F.F. Hou, G.B. Wang, F. Yang, D. Xie, Y.P. Wang, J.W. Tian, Accumulation of advanced oxidation protein products induces podocyte apoptosis and deletion through NADPH-dependent mechanisms, Kidney Int 76 (2009) 1148–1160.
[104] A. Żyłka, P. Dumnicka, B. Kuśnierz-Cabala, A. Gala-Błądzińska, P. Ceranowicz, J. Kucharz, A. Ząbek-Adamska, B. Maziarz, R. Drożdż, M. Kuźniewski, Markers of glomerular and tubular damage in the early stage of kidney disease in type 2 diabetic patients, Mediat. Inflamm. 2018 (2018) 7659243.